AD NUMBER

**ADB009131**

LIMITATION CHANGES

TO:

**Approved for public release; distribution is unlimited.**

FROM:

**Distribution authorized to U.S. Gov't. agencies only; Test and Evaluation; JAN 1976. Other requests shall be referred to Army Electronics Command, Fort Monmouth, NJ.**

AUTHORITY

**ECOM ltr 10 Mar 1977**

Research and Development Technical Report
Report ECOM-72-0297-F



# RADIATION AND THERMALLY HARDENED SWITCHING MATERIALS

**SOO H. SHIN and PAUL M. RACCAH**

**YESHIVA UNIVERSITY**
**BELFER GRADUATE SCHOOL**
**MAYBAUM INSTITUTE**
**2495 AMSTERDAM AVENUE**
**NEW YORK, NEW YORK 10033**



JANUARY 1976
*FINAL REPORT for period*
July 1972 to 30 June 1975





Prepared for
**ECOM**
US ARMY ELECTRONICS COMMAND FORT MONMOUTH, NEW JERSEY 07703

HISA FM 2958-73

# NOTICES

## Disclaimers

The findings in this report are not to be construed as an official Department of the Army position, unless so designated by other authorized documents.

The citation of trade names and names of manufacturers in this report is not to be construed as official Government indorsement or approval of commercial products or services referenced herein.

## Disposition

Destroy this report when it is no longer needed. Do not return it to the originator.

UNCLASSIFIED

SECURITY CLASSIFICATION OF THIS PAGE (When Data Entered)

## REPORT DOCUMENTATION PAGE

READ INSTRUCTIONS BEFORE COMPLETING FORM

| | |
|---|---|
| 1. REPORT NUMBER: ECOM-72-0297-F | 2. GOVT ACCESSION NO. |
| 3. RECIPIENT'S CATALOG NUMBER | |
| 4. TITLE (and Subtitle): RADIATION AND THERMALLY HARDENED SWITCHING MATERIALS. | 5. TYPE OF REPORT & PERIOD COVERED: Final Report. 1 July 1972 to 30 June 1975 |
| | 6. PERFORMING ORG. REPORT NUMBER |
| 7. AUTHOR(s): S.H. Shin and M. Raccah | 8. CONTRACT OR GRANT NUMBER(s): DAAB07-72-C-0297 |
| 9. PERFORMING ORGANIZATION NAME AND ADDRESS: Belfer Graduate School of Science - Yeshiva U. 2495 Amsterdam Avenue New York, N.Y. 10033 | 10. PROGRAM ELEMENT, PROJECT, TASK AREA & WORK UNIT NUMBERS: Project No. 1S762705AH94 Task No. W3 Subtask No. 01 |
| 11. CONTROLLING OFFICE NAME AND ADDRESS: U.S. Army Electronics Command Fort Monmouth, New Jersey 07703 (AMSEL-TL-MD) | 12. REPORT DATE: January 1976 |
| | 13. NUMBER OF PAGES: 52 |
| 14. MONITORING AGENCY NAME & ADDRESS (if different from Controlling Office): DA-1-S-762705-AH-94 | 15. SECURITY CLASS. (of this report): Unclassified |
| | 15a. DECLASSIFICATION/DOWNGRADING SCHEDULE |

16. DISTRIBUTION STATEMENT (of this Report) 1-S-762705-AH-94-W3.

Distribution limited to U.S. Government agencies only, Test and Evaluation, January 1976. Other requests for this document must be referred to Commander, U.S.Army Electronics Command. ATTN: AMSEL-TL-MD, Fort Monmouth, N.J. 07703.

17. DISTRIBUTION STATEMENT (of the abstract entered in Block 20, if different from Report)

18. SUPPLEMENTARY NOTES

19. KEY WORDS (Continue on reverse side if necessary and identify by block number)

Switching
Niodium dioxide
Spike suppressant
Semiconductivity

20. ABSTRACT (Continue on reverse side if necessary and identify by block number)

The field switching properties of $NbO_2$/$NbO$,$NbO_2$/(reduced $NbO_2$) and polycrystalline nonstoichiometric $NbO_2$ have been investigated. Under an applied electric field they switch from a high (> 10 KΩ) to a low (~ 10 Ω) resistance in times smaller than 0.7 ns. For pulse durations of several nsec, the current carrying capability is higher than 80 A. The switching mechanism appears to proceed in two stages which could be electrode limited Schottky barrier breakdown and bulk limited field lowering process of $NbO_2$, then followed by a thermal runaway.

DD FORM 1 JAN 73 1473 EDITION OF 1 NOV 65 IS OBSOLETE

UNCLASSIFIED 053 820

SECURITY CLASSIFICATION OF THIS PAGE (When Data Entered)

CONTENTS

## Figure Captions

## List of Tables

## I. INTRODUCTION

Our aim has been to prepare and study materials in order to achieve more reproducible homogeneous single and polycrystalline materials capable of high speed switching between low and high conductive states. The low mobility of transition metal oxide insulators makes them excellent candidates. However, we had to avoid materials (such as $VO_2$) which undergo a first-order phase transition at a certain critical temperature with a concomitant structural transformation. A way around this problem was to find materials undergoing a large mobility and band structure transformation without a drastic change in the basic lattice symmetry. Such is the case of $Ti_2O_3$, which was reported on at the first stage of this program. Our results on $Ti_2O_3$ showed the possibility of field switching materials which undergo a semiconductor-to-metallic transition only at liquid He temperature. Consequently, the next logical step appeared to be to choose a material which undergoes a semiconductor-to-metallic transition at a temperature much higher than $Ti_2O_3$ because it would have fewer free carriers to cool and freeze out free carriers.

Niobium dioxide, $NbO_2$, was chosen as a next candidate for this investigation since it has a second order semiconductor-to-metallic phase transition at 1070°K. The electronic carriers have a low, anisotropic mobility at all temperatures. It was shown that the mobility in the low temperature phase ($< 1070^{\circ}K$) could be described in terms of small polarons. This indicates a localization of the single 4d electron of the $Nb^{+4}$ ions via a pairing along the c-axis, stabilized by a lattice distortion. After we failed to switch bulk $NbO_2$ single crystal, we were able to develop radiation hard $NbO/NbO_2$ devices capable of shunting transient currents spikes of up to 80 Amp in times shorter than resolution of the apparatus (0.7 ns). We report here on the

preparation methods and physical properties of $NbO_2$ thin film on NbO substrate (Section II) and thinned stoichiometric $NbO_2$, which has a similar characteristic to $NbO/NbO_2$ devices (Section III). Section IV describes non-stoichiometric effects on $NbO_2$ single crystal under DC field, as well as intense pulse fields in order to establish the mechanism of switching. We have also attempted to relate the mechanism to physical measurements on transport and structural properties, particularly nonstoichiometric effects on $NbO_2$ single crystal. Based on various experimental evidence, which includes scanning electron microscopy, we must improve the longevity and severe damage of our devices. Finally, Section V describes the polycrystalline form of devices ($NbO_{1.87}$) which demonstrated further experimental evidences to meet the specific requirement of radiation and thermally hardened switching material for devices. The summary shows a natural substitute for the more sophisticated single crystal technique and promises remarkable speed and power handling capabilities of new devices.

## II. $NbO_2$ FILM ON NbO SUBSTRATE (A-TYPE DEVICES)

### 1) INTRODUCTION

A systematic analysis of the results obtained in the previous work periods of the ongoing contract led to the conclusion that the switching phenomena originally observed in needle shape crystals could not have been the bulk properties of $NbO_2$, doped or not. Instead it occurred to us that very high fields are needed and therefore we should try thin films of $NbO_2$ on conducting substrates.

### 2) SAMPLE PREPARATION OF NBO/$NbO_2$

The NbO chips used in the course of the present investigation are prepared by Czochralski-Kyropoulos technique. The method used is the reaction of intimately mixed niobium (Nb) and niobium pentoxide ($Nb_2O_5$) powders in the tri-arc furnace, according to reaction (1)

$$3\ Nb + Nb_2O_5 \rightarrow 5\ NbO \qquad (1)$$

The procedure followed was to press into pellets appropriately weighed powder mixtures of Nb metals (9.291 g) and $Nb_2O_5$ (8.861 g). Analysis of the starting materials by spectroscopic techniques showed the following impurities in the part per millions:

- For Nb metal  Ta $<$ 100,  Fe $\sim$ 2,  Ca $<$ 1
- For $Nb_2O_5$  Ta $<$ 50 ,  Si $<$ 1, Ca $<$ 1, A$\ell$ $<$ 1 .

The pellets were then placed in the water cooled rotating graphite hearth of the furnace and electric arcs struck to them. This melted and reacted on the powder mixture in a circulating atmosphere of purified argon with a measured oxygen content less than 10 ppm. Under these conditions NbO appears to melt congruently (melting point of NbO: 2218°K), and the low resistance of the melt makes it very easy to maintain stable arcs which heat

the rotating melt uniformly. This technique[1] is effectively crucibless since the bottom of the melt, in contact with the cooled graphite hearth, is solidified and forms its own crucible minimizing contamination. In order to grow crystals, a tungsten tip, attached to the heat pipe pulling rod was immersed into the melt and a fine neck produced by retracting and positioning it. Typically, the crystals were pulled at a rate of 2 inches per hour. However, when the seed crystal was used, it was possible to grow large crystals, typically 1 x $\frac{1}{4}$ inches. A typical crystal is shown in Fig. 1.

The stoichiometry of the niobium to oxygen ratios was determined by reoxidizing a known weight of the sample to $Nb_2O_5$. The stoichiometry ratios used are quite close to $NbO_{1.00}$ accurate to within 0.5 atomic percent. The resistivity of the typical sample is $1.21 \times 10^{-5}$ ohm-cm at 300°K. We have compared its resistivity to that given in previously published data for material of the same composition. Our results are in reasonable agreement with Chandrashekhah's measurements[2]. The resistivity is very low and comparable to that of the element Nb from which the oxide is derived. Since NbO single crystal has a rock salt structure and cleaves very well, this NbO grown by Czochralski's technique can be cleaved into thin wafer $\frac{1}{3}$ to 1/10 mm. thickness using razor blades. Small NbO chips, typically 1 x 1 x 0.5 mm in dimension, were heated in the presence of a large amount of $NbO_2$ powder in vacuum and at various temperatures. When the chips were oxidized under partial oxygen pressure of $NbO_2$, it proved easier to form $NbO_2$ on NbO surface if small amounts of $Nb_2O_5$ powder were added into $NbO_2$ powder. For example, 2 g. of NbO chips, 0.1 g. $Nb_2O_5$ (~ 1% $Nb_2O_5$ of total NbO chips) and 8 g. of $NbO_2$ powder prepared freshly were sealed in a quartz ampoule and heated approximately for 24 hours at 850°C. Then an $NbO_2$ layer was formed all over the surface of NbO chips. The thickness of the $NbO_2$ film varies from 1 to 10 μ approximately. (See Figs. 3 and 4).

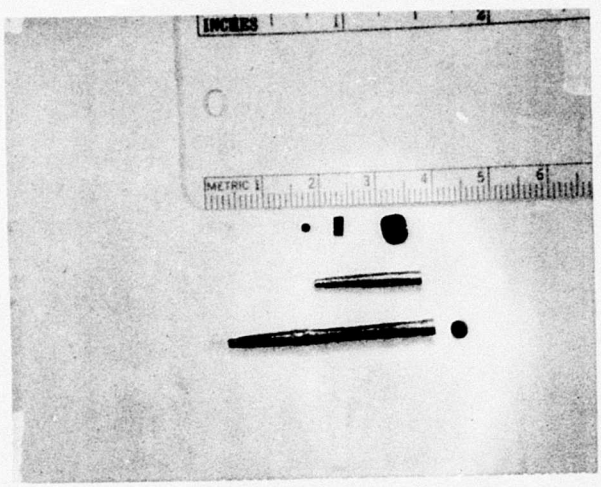


Fig. II - 1

Typical NbO single crystal and cleaved NbO chips

3) FILM STRUCTURE

In order to establish conclusively the nature of the $NbO_2$ coating which was formed on the NbO chips, we performed two tests. A first test was to run an X-ray diffraction pattern and the other was to examine a pure NbO crystal and a sample of $NbO_2$ films by ESCA.

The diffraction pattern of the prepared material was in good agreement with Magnelli's powder pattern of $NbO_2$ sample. Fig. 2 shows the diffraction pattern of the $NbO_2$ films on NbO chips. A faint foreign line is observed which is probably due to NbO. This in itself is quite convincing. In addition, the resistivity measurements indicate an $NbO_2$ thickness of $\sim 1$ μm, which is confirmed again by scanning electron microscopy (SEM).

ESCA measurements show a thin layer (15 to 20 Å) of $NbO_2$ present in the virgin cleaved NbO starting material. This indicates, consistently with other works, that the first higher Nb oxide is $NbO_2$. Furthermore, the ESCA spectra of our $NbO_2$ film turned out to correspond exclusively to $NbO_2$. After oxidation, the ESCA spectra showed the peaks shifting in energy, presumably due to changes in the surface to volume ratio of the polycrystalline oxide growth. Therefore both X-ray and ESCA show that the layer formed on NbO substrate is only $NbO_2$, confirming that there is no intermediate state between $NbO/NbO_2$. Furthermore, there is no higher oxidation state, $Nb_2O_5$.

We also confirmed this switching in an $NbO_2$ single crystal. An $NbO_2$ single crystal piece was lapped down to a thin layer,and annealed under vacuum or $H_2$ and Ar gas to produce a conducting surface as well as to reduce further the thickness of the specimen. The conducting edge of specimen was cut off from the sample. When the electric field was applied, we could get the same switching behavior, except a threshold voltage a little bit higher than with the $NbO_2$ thin film.

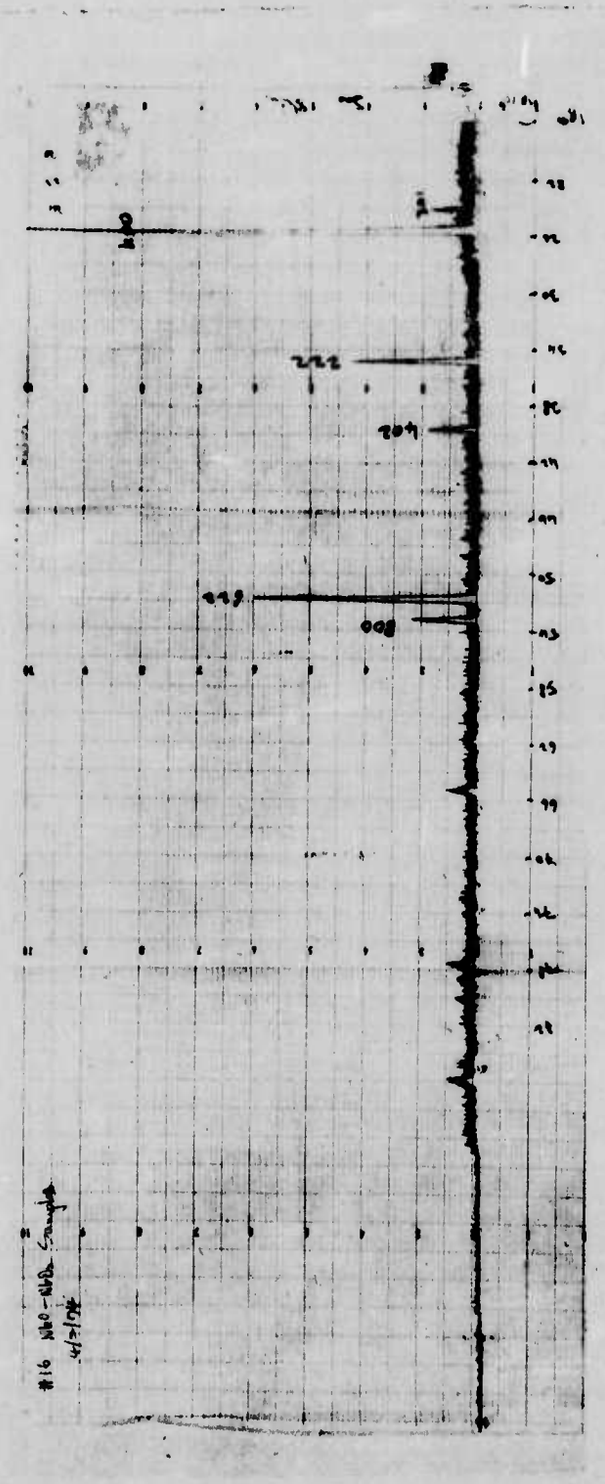


Fig. II - 2

X-ray diffraction patterns of $NbO_2$ film formed on NbO substrate

In order to study microscopic structure of the $NbO_2$ film and the relation between the DC resistance and film thickness, a few samples with different DC resistance were sent to Electronics Technology and Devices Laboratory, USAECOM, Fort Monmouth, N.J. for examination by Scanning Electron Microscope (SEM) techniques. Based on these SEM results, the following facts were recognized:

1) The thickness of a device with 50 Ω of DC resistance turns out to be 0.1 μm thick, and NbO substrate was covered with a very fine grain of polycrystalline $NbO_2$.

2) The thickness of 18 KΩ-device was found to be 1 μm thick, which was consistent with the estimated value by resistivity measurements. (See Fig. 3-A). The $NbO_2$ layer formed on the NbO single crystal was a larger grain size and was preferentially oriented perpendicular to surface of the substrate (See Fig. 3-B).

3) The $NbO_2$ layer of 130 KΩ device was 6.6 μm thick (Fig. 4-A) and well defined spots were interconnected and the grain size became reduced to ~ 0.1 to 0.2 μm (Fig. 4-B).

These results indicate that the DC resistance is proportional to its thickness of $NbO_2$ layer and a low resistance sample would be easily shorted with a few pulses due to a poorly formed structure.

## 4) CHARACTERISTICS OF NbO/$NbO_2$ DEVICES

The chips obtained by the technique described above were placed for preliminary testing on a rhodiated copper plate, making contact on one side, and the assembly was completed by applying a pressure contact via a gold ball point (0.5 mm diameter) on the other side. Pulses of 0.1 μsec. duration

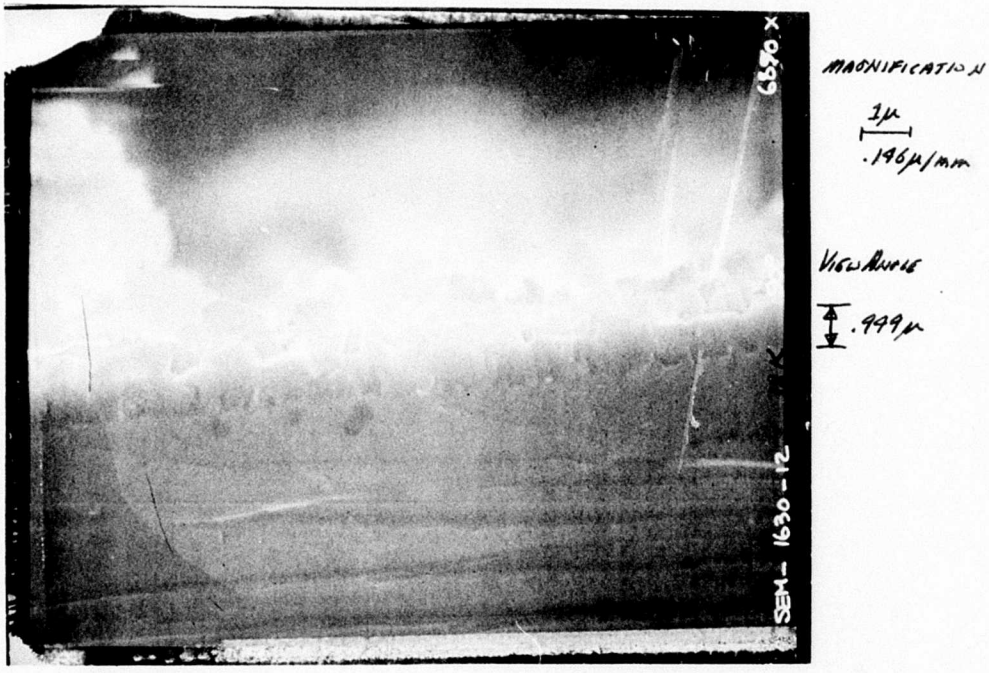


Fig. II - 3(A)

Scanning electron microscope (SEM) photograph showing 1 μm thick $NbO_2$ layer grown on NbO substrate

#624
18K

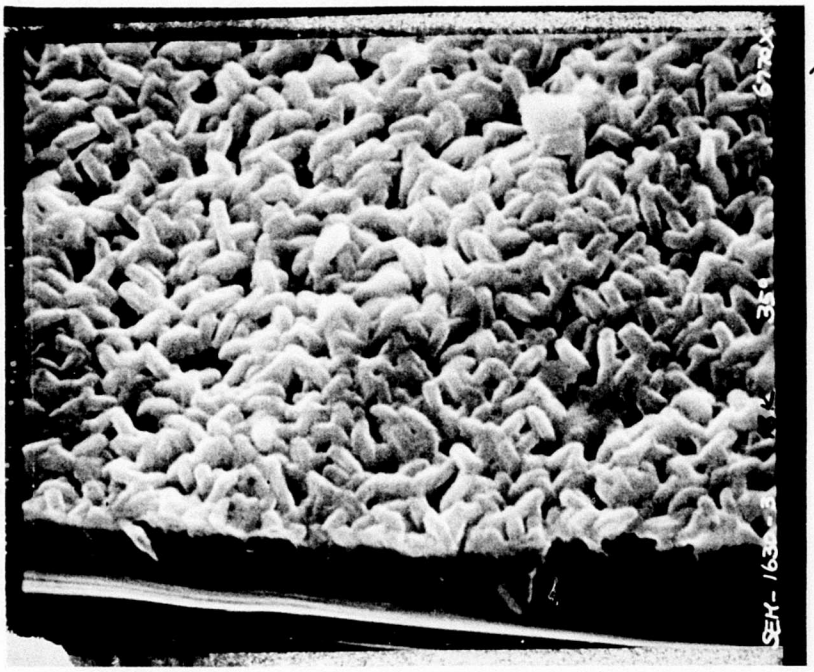


Fig. II - 3(B)

SEM photograph showing $35^{o}$ angle view and columnar growth pattern of polycrystalline $NbO_2$

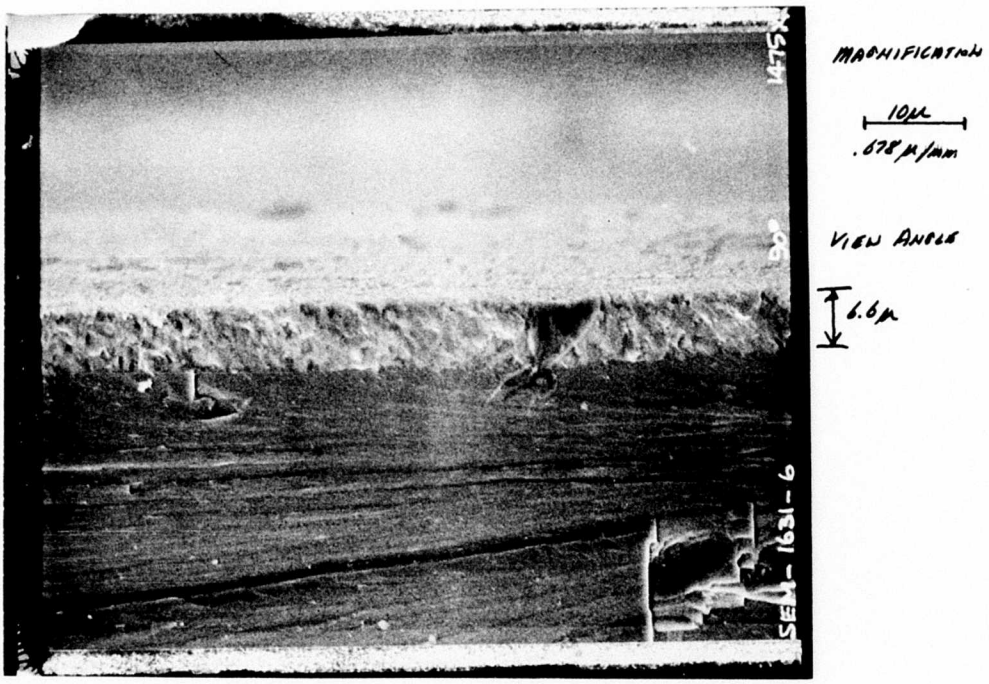


Fig. II - 4(A)

SEM photograph showing an edge-on view of a cleaved device of which $NbO_2$ oxide layer is 6.6 μm

#711-1
130K,

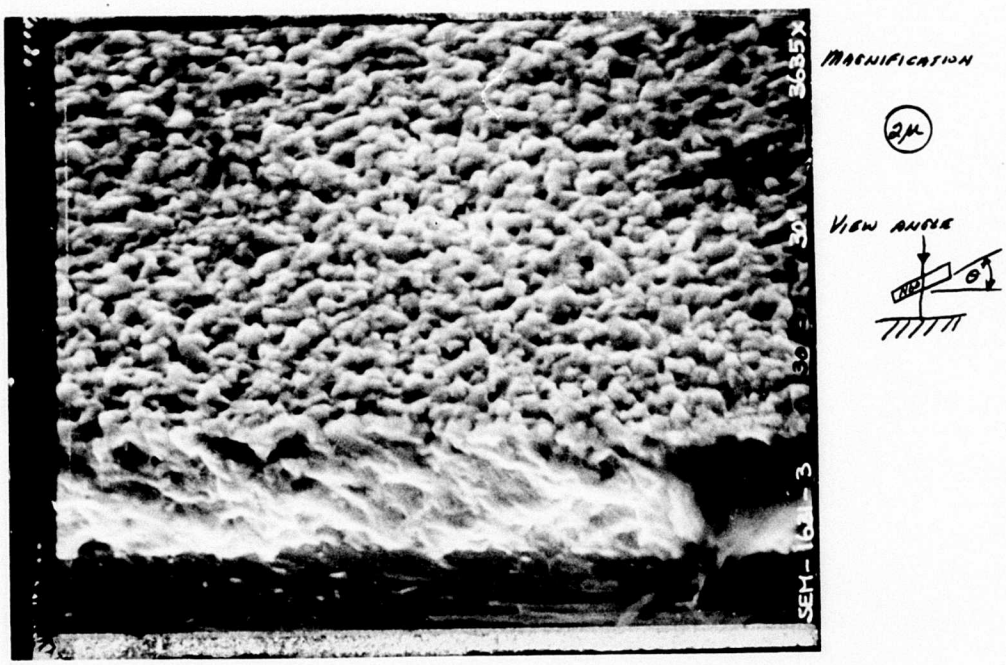


Fig II - 4(B)

SEM photograph showing that well defined spots were interconnected comparing Fig. II-3(B)

and 30 ns risetime were delivered by a Velonex model 350 pulse generator at a rate of 1 Hz.(Fig.5). The pulse's voltage was increased slowly while the sample response was followed on an oscilloscope in order to find the critical voltage at which it would switch. Typically, for a pure $NbO_2$ layer of thickness ranging from 1 to 10 μm,the off resistance measured with a D.C. multimeter varied from a few kilcohms to several ten kiloohms, but the threshold voltage did not change significantly and was of the order of 120 to 150 volts. The capacitance, measured at $10^6$ Hz in the sample holder described above, was found to vary from 0.5 to 1.0 pF.

Furthermore, our effort has been directed towards packaging of the existing devices as well as systematization of production procedures. After discussion with Capt.Laplante of USAECOM, we have tried one microwave diode package presently available on the market. The motivation is obvious since microwave diode packages are designed to minimize capacitance and induction. It is also clear that the problems encountered in building microwave diodes are quite similar to the problems we ourselves are encountering. While we are not too enthused with the fact that these packages are point contact systems, we do feel however that it was an improvement on the pressure contact situation. The use of one of the packages turned out to be quite practical.

Finally, one of the stabler configurations was obtained using standard 1N23 (X-band) microwave diode packages (Fig. 6), manufactured by Microwave Associated International, Inc. Burlington, Mass. Because in this package the point contact is made by a spring loaded tungsten whisker the contact area is smaller and the off resistance of our devices varied, depending on the $NbO_2$ layer's thickness, between 20 and 500 KΩ, as measured with a D.C. multimeter.

The threshold voltage was found to vary from 130 to 260 volts and the capacitance measured at $10^6$ Hz was of the order of 0.5 pF.

In order to find out how well these devices would respond to fast risetime and high current (80 A ) pulses, they were tested by Cpt.Laplante, USAECOM, Fort Monmouth, N.J., using a 50 Ω cable discharge pulser capable of output voltages up to 2000 V. The device response was photographed using a Tektronix 7904 oscilloscope with high speed writing capability and a maximum aperture camera system. This equipment allowed 0.7 ns risetime resolution of single shot pulses. Contrary to previous experience with other switching materials, such as amorphous semiconductors, no delay could be observed and within the limit of resolution ($\leq$ 0.7 ns) the response of the device to the incident pulse appeared instantaneous. However, in amorphous switching, the device, once it did switch, traversed the negative resistance path on the I vs. V characteristic nearly instantaneously. In our devices, this post-switching negative resistance path is traversed in a measurable time with an 80% reduction in voltage in the first 10 ns. This was taken to indicate that the switching proceeds in two stages, the first one being electronic in nature and occuring in the first nanosecond while the second was a non-destructive thermal runaway resulting in filamentary high current density conduction. The second stage has long been known to occur, in materials such as $NbO_2$ which are capable of undergoing a semiconductor to metallic phase transition, if sufficient energy is dissipated in the form of Joule heating.

The maximum current tolerated by the devices was 80 A for pulse durations of 15 ns using the cable discharge pulser with the corresponding cable. A maximum current of 80 A for the maximum pulse duration of 160 ns, obtained using the longest cable, was also successfully tolerated by the device. In an attempt to investigate longer duration pulses, a Cober 605 P high power

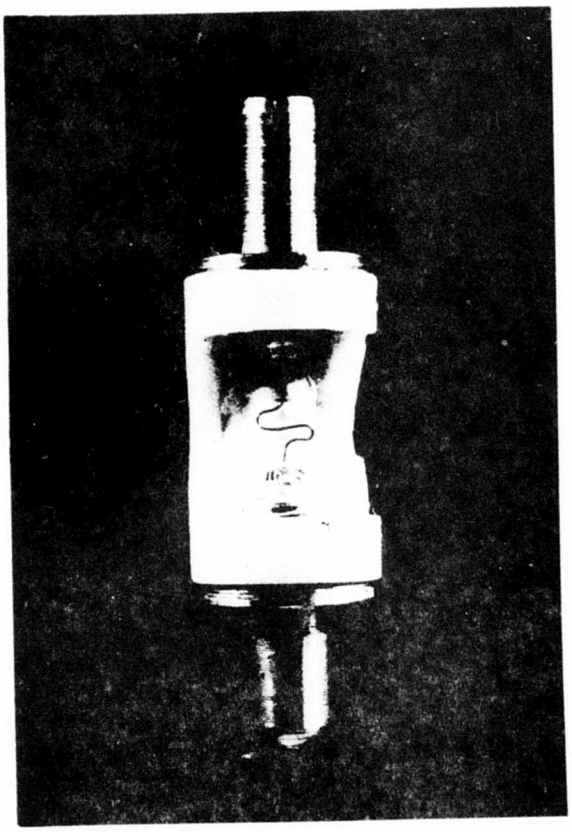

Fig. II - 6

Standard X-band 1N23 microwave diode package A-type device is mounted with tungsten whisker contact

pulser was used to apply up to 3 ms single shot pulses at its maximum current of 11 A. The addition of an appropriate pulse transformer allowed the application of 1.0 μs duration pulses at a maximum current of 22 A. These results are reported fully elsewhere.[3]

Some results of these specimens tested by Cpt Laplante are summarized in Table 1. Based on these results, which include scanning electron microscopy done by Mr. Charles Cook of the Electronics Technology and Devices Laboratory, U.S. Army Electronics Command, Fort Monmouth, N.J.:

a) The tungsten whisker making pressure contact in the diode packages was considerably eroded after a few pulses (2000 volt) indicating that high temperatures are reached by the tip. (See Fig. 6).

b) During pulsing the $NbO_2$ layer oxidizes in the contact areas because of the high temperatures developed.

Potting the assembly electrodes/chip in the diode package with 5 minute epoxy from Devcon Corp. appeared to be the simplest solution. We found that the typical off resistance of a potted device was of the order of ~ 150 KΩ. During pulsing (1 Hz, 630 volts pulse amplitude and 0.1 μsec. pulse width), the off resistance would increase to 20 MΩ and then would completely open after a few hours. Given the erosion of the tungsten contact shown by the SEM pictures after repeated pulsing, it was reasonable to assume that the epoxy prevented the spring action forcing a gap to form, and inducing open circuit failure.

Indium has a low melting point but a high boiling temperature. We decided to place a bead of In at the end of the tungsten whisker. Heat would

TABLE II-1

Switching Characteristics of $NbO_2/NbO/NbO_2$ (A-type) Devices

| Devices | $I_p$ (MA) | $V_p$ (volts) | $V_{th}$ (volts) | $V_{th}$ (volts) | $R_{30mhz}$ (KΩ) | $C_{30mhz}$ (pf) |
|---|---|---|---|---|---|---|
| A-1 | 1.0 | 14 | 250 | 250 | 17.9 | 0.37 |
| A-2 | 0.8 | 36 | 700 | 180 | 14.1 | 0.33 |
| A-4 | 1.0 | 40 | 460 | 300 | 7.9 | 0.44 |
| A-5 | 1.0 | 50 | 640 | 380 | 22.7 | 0.41 |
| A-6 | 1.3 | 34 | 300 | 100 | 9.2 | 0.50 |
| A-9 | 1.2 | 25 | 100 | 70 | 25.2 | 0.60 |
| A-11 | 1.0 | 16 | 90 | 80 | 7.4 | 0.40 |
| Average | 0.90 | 31 | 360 | 194 | 14 9 | 0.44 |

Note

1) Specimen were mounted in 1N23 diode package and contact was made with tungsten whisker.

2) The threshold voltage was determined by minimum voltage needed to switch a device for a 1 ns pulse width.

3) $I_p$ and $V_p$ were measured in a curve tracer.

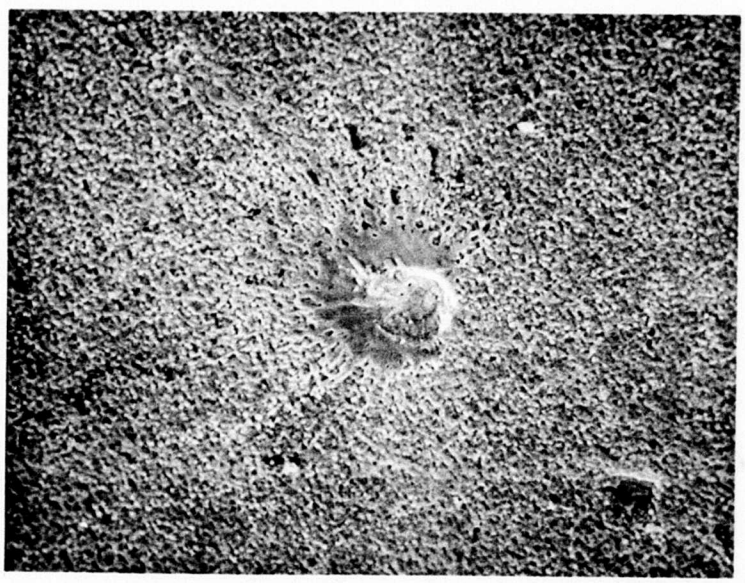

Fig. II - 6

The eroded $NbO_2$ layer after a few 2000 volts pulses while contact was made with tungsten whisker

only melt the In and insure a better contact. Now the In induced short circuit failure in the case of $NbO_2$ film on NbO substrate. However in the case of thin $NbO_2$ single crystal layer described in the next section, the results were quite satisfactory.

5) B-TYPE DEVICES

Attempts have been made at trying to develop a low voltage device by producing a different type of configuration . Instead of $NbO/NbO_2$, we have attempted to make $TiO/Ti_3O_5$ devices. The method used was exactly the same as for the standard $NbO/NbO_2$ spike suppressors, i.e., we have annealed chips of TiO single crystals in sealed ampules in the presence of an excess $Ti_3O_5$ powder. This process was successful and we did obtain a coating of $Ti_3O_5$ on the TiO chips. The devices did switch at relatively low voltage compared to the $NbO/NbO_2$ devices. These devices are based on a configuration between a conducting substrate and an oxide which can undergo a semiconductor to metallic transition (SCM). Example: NbO (metallic)/$NbO_2$ (SCM at 807°C) or TiO (metallic)/$Ti_3O_5$ (SCM at 135°C). We also have tried $VO/VO_2$ and it does work. However the off resistance is somewhat low and the device fragile because of the closeness to the actual transition temperature (SCM at 65°C).

6) $NbO_2$ FILM ON NIOBIUM METAL SHEET

In order to confirm experimentally the possibility of using Nb-metal for device fabrication, we have performed measurements using $NbO_2/Nb/NbO_2$ thin film devices. This turned out successfully and would certainly be a cheaper approach to device construction. Since niobium metal exposed to an oxidizing atmosphere would first form NbO, and then $NbO_2$, we would necessarily get the same $NbO/NbO_2$ configuration on top of an Nb electrode which should be no problem. The only question was whether the general grain structure of the successive layer would turn out to be too fragile for repeated pulsing.

TABLE II-2

Switching Characteristics of B-type Devices

| | $NbO_2/NbO$ | $Ti_3O_5/TiO$ | $VO_2/VO$ | |
|---|---|---|---|---|
| $T_{SCM}$ (°C) | 807 | 135 | 65 | Sem. to metallic transition temp. of semiconducting oxide |
| $V_{th}$ (volt) | 130 | 50 | 2 ~ 5 | 0.1 μsec pulse width from Velonix |

Commercially available Niobium foil, 0.25 mm. thick, 99.99% pure, produced by Ventron Chemical Co. was cut into 2x2 mm. pieces, and then oxidized with partial pressure of $NbO_2$ powder at 900°C. The characteristics of this device are similar to that of the $NbO/NbO_2$ configuration; the off resistance (DC) was typically of the order of 30 KΩ and the device switched at ~ 85 volt, with 0.1 μ pulse width. Longevity tests have shown that the devices are somewhat more fragile than those produced from NbO single crystal chips.

7) Ti-DOPING EFFECT ON NbO SINGLE CRYSTAL SUBSTRATE.

Ti-doping was introduced in the original NbO single crystals on which the $NbO_2$ layers are grown. In this way, as $NbO_2$ is formed by oxidation, it is automatically doped by the Ti present in the proper portion. Its purpose was to improve the switching characteristics through reducing the energy gap and therefore the threshold voltage. In fact, the purpose of this doping was triple:

a) It is hoped that Ti-doping reduces the oxygen affinity because Ti cannot be oxidized to the 5+ state, and therefore improves the lifetime of our devices.

b) Ti-doping prevents fast dendritic growth also due to the high oxygen affinity for NbO.

c) Ti-doping reduces the band gap and therefore the potential barrier to switching.

EXPERIMENTAL RESULTS

We have performed an experimental investigation on Ti-doping effect on NbO single crystals. Ti-doped NbO single crystals, $Nb_{1-x}Ti_xO$, with $0 \leq x \leq 0.1$ have been grown successfully and we have compared their switching characteristics to undoped $NbO/NbO_2$ thin film devices.

The Ti-doped NbO single crystals were prepared by addition of Ti metal (99.99%) or $TiO_2$ (99.995%) to the appropriate amounts of Nb and $Nb_2O_5$ mixture, as described in section II.

Various Ti-doped NbO chips were sealed in a quartz ampoule with enough $NbO_2$ powder, and then oxidized at 900°C for about 20 hours. The specimens were mounted between a rhodiated copper plate and a gold ball point (0.5 mm diameter). The threshold voltage was determined by using 0.1 μsec pulse width. The results were quite satisfactory, except for a low off resistance. The observed switching voltage decreased almost exponentially with x for doping concentration of titanium. The layers looked at by scanning electron microscopy proved to be considerably more dense and uniform than previously. Fig. 7 shows the effect of Ti-doping for the threshold voltages. A 10% Ti-doped thin film device switched at lower than 20 volts compared with switching voltages to ~ 85 volt of the undoped thin film device.

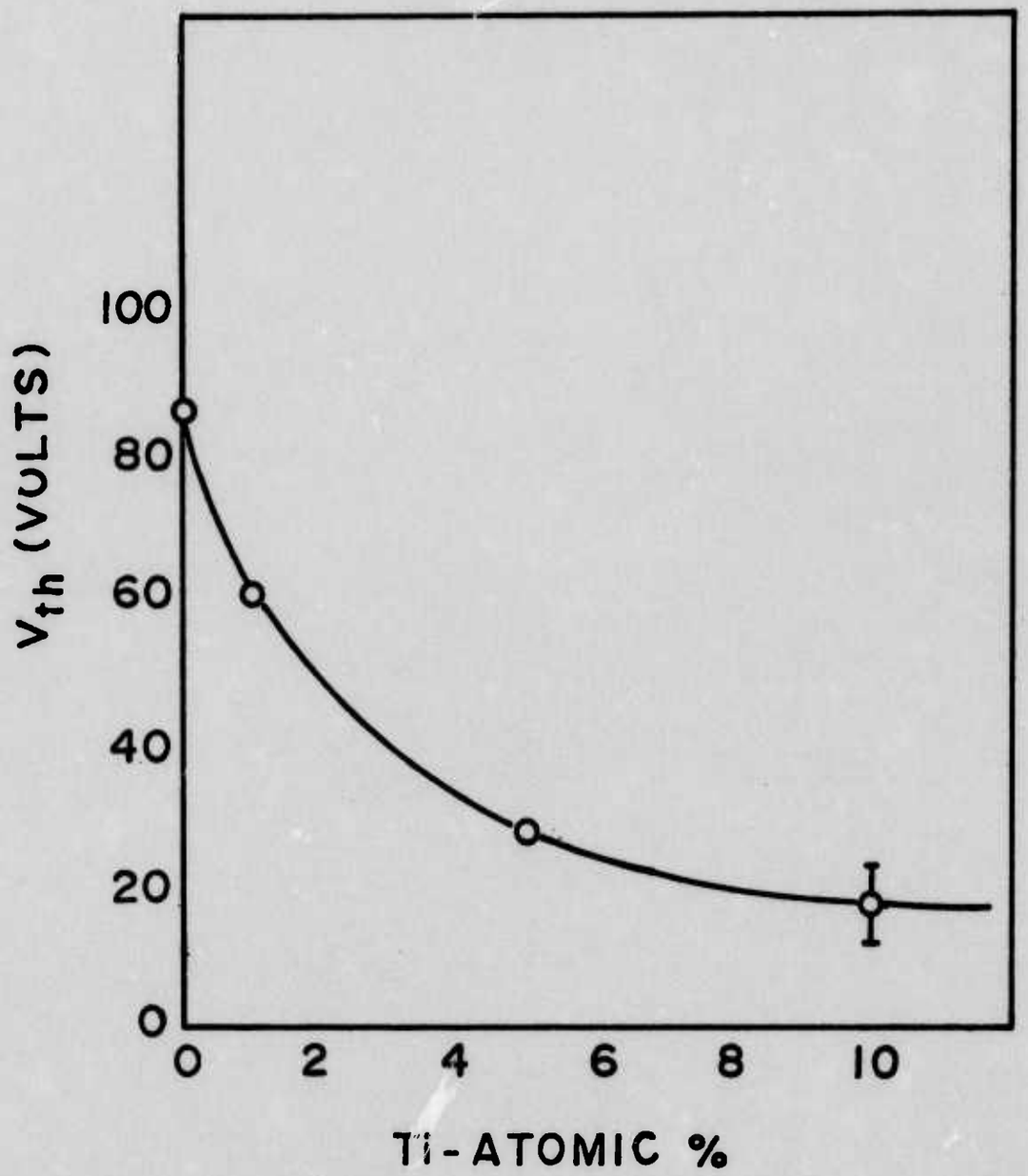


Fig. II-7

Threshold voltages vs. Ti-doping in $NbO_2/NbO/NbO_2$. Threshold voltages decreases exponentially with Ti-Atomic % in $NbO_2/NbO/NbO_2$ devices.

## III. THINNED $NbO_2$ SINGLE CRYSTAL DEVICES (C-TYPE DEVICES)

### 1) BACKGROUND INFORMATION.

At the first stage of this program we succeeded in obtaining $NbO_2$ materials behaving as transient suppressors with high switching speeds, low trigger voltages and high current capability. However, when we prepared a better quality of $NbO_2$ single crystals, it gave negative results. Since then, our work has addressed itself mainly to the preparation of thin layers (1 to 10 μm) of $NbO_2$ on NbO single crystal chips described in detail in Section II. It would appear that in fact we did not switch in the original materials the bulk, but rather some layers of $NbO_2$ upon a conducting substrate of non-stoichiometric $NbO_2$ like $NbO_{1.87}$, which is described in the next sections. How this came about in the original preparation has not yet been elucidated but we are taking steps to test the switching of $NbO_2$ under intense fields by means of making thin single layers on a conducting substrate.

### 2) PREPARATION OF THIN LAYER OF $NbO_2$ CRYSTAL

While we were able to establish that the switching element is indeed the pure $NbO_2$ layer, the physical structure of that layer has become a point of interest because of the need to develop good electrode contact. More recently we have attempted to prepare $NbO_2$ single crystal chips thin enough to be switched. Since it is usually impossible to thin down a single crystal to the size of even 10μ we proceeded in the following manner: we lapped down an $NbO_2$ single crystal to the thickness of approximately 0.1 mm then further decreased the effective thickness by reducing the surface. As we have already reported, reduced $NbO_2$ had a lower conductivity than pure $NbO_2$, hence the crystal surface once reduced became a very good electrode. It was possible to switch the single crystal chip. The threshold voltage turned out to be the well known ~ 300 volts with 0.1 μs pulse width. We

intended to further develop this approach because obviously this single crystal technique presents excellent electrode contact possibilities. We have since learned through experience that the $NbO_2$ layers produced by surface oxidation of NbO single crystals are fragile when submitted to long pulses (over 10 μsec pulse width). The advantage of $NbO_2$ single crystal devices are double, for one thing $NbO_2$ single crystals are considerably more resistant to oxidation because the existing surface is very small. For another, $NbO_2$ single crystals are flat and smooth which makes for very good electrode binding properties. We found that it was necessary to thin down a single crystal plate to a thickness of a few mils. When we made contact directly with Ag-paste and a screw in regular microwave diode package, the switching voltage was very high, of the order of 300 to 330 volts with a 0.1 μ pulse. These specimen were forwarded to USA ECOM for testing. Some results provided by Cpt. Laplante are summarized in Table 3. The capacitance as measured by Cpt. Laplante turned out to be 2 pF which is only 3 to 4 times larger than our regular $NbO_2/NbO/NbO_2$ devices.

When contact was made, using tungsten whiskers with Indium and potted in epoxy, the results were similar but we found that devices were stable. It turned out that the I vs. V characteristic in these new types of devices is extremely reproducible and stable. These types of devices with proper contacts should be able to handle much larger currents and we have already checked that they can handle very long (100 microseconds) pulses.

Table III-1

Switching Characteristics of Thinned $NbO_2$ single Crystal

| | $I_p$(MA) | $V_p$(volts) | $V_{th}(1)$ | $V_{th}(2)$ | $R_{30mhz}$ | $C_{30mhz}$ |
|---|---|---|---|---|---|---|
| C-11 | 4.4 | 7.0 | 130 | 110 | 4.9 | 1.75 |
| C-12 | 6.0 | 18 | 400 | 450 | 5.2 | 3.10 |
| C-13 | 2.2 | 18 | 320 | 330 | 6.7 | 2.27 |
| C-15 | 3.6 | 13 | 220 | 230 | 7.8 | 0.77 |
| C-16 | 4.2 | 76 | 400 | 420 | 10.5 | 1.74 |
| C-17 | 12.0 | 7.0 | 350 | 350 | 4.0 | 1.26 |
| Average | 5.40 | 12.6 | 303 | 350 | 6.9 | 0.85 |
| C-14 | 4.0 | 17 | 350 | 350 | 6.9 | 0.85 |

Note

1) The first series of specimen are epoxied, indium contacted to sharpened set screw.

2) The threshold voltage was determined by minimum voltage needed to switch a device for a 1 ns pulse width.

3) $I_p$ and $V_p$ were measured in a curve tracer.

## IV. NON-STOICHIOMETRIC EFFECT ON $NbO_2$ SINGLE CRYSTAL

### 1) OBJECTIVES

Our purpose has been to study more systematically high quality single crystals of $NbO_2$ under DC field as well as intense pulse fields in order to establish the mechanism of switching. We have in particular attempted to relate the mechanism to physical measurements on transport and structural properties, particularly the non-stoichiometric effect on $NbO_2$ single crystal.

### 2) INTRODUCTION

Niobium dioxide, $NbO_2$, has a second order semiconductor-to-metallic (SCM) transition at 1070°K. Belanger et al. studied the transport properties of stoichiometric single crystal $NbO_2$, and demonstrated that the mobility in the low temperature phase ($T < 1070^{\circ}K$) could be described in terms of small polaron

Considerable amount of work on controlled stoichiometric $NbO_2$ has been done in our laboratory. A large portion of this work concerned a study of single crystal $NbO_x$ with $1.90 \leq x \leq 2.10$ and polycrystalline $NbO_{1.87}$. The latter material is studied in detail in the next section.

Jannick and Whitmore studied the transport properties in relation to the materials stoichiometry. They reported a very narrow range of non-stoichiometry ($2.003 \geq 1.997$) for $NbO_x$ hardly affecting the transport mechanism. In the process of growing stoichiometric $NbO_2$ single crystals for various studies, we were led to question whether Jannick and Whitmore's claim of a very narrow compositional range of existence implied that a stoichiometric crystal could be pulled from a non-stoichiometric melt. This turned out not to be the case, and our Laue and thermogravimetric studies indicated that we could grow perfectly well defined large single crystals of composition $1.90 \leq x \leq 2.10$ in contrast with Jannick and Whitmore's result of $1.997 \leq x \leq 2.003$ obtained on powders.

3) STOICHIOMETRIC $NbO_2$ and $Nb_{1-x}Ti_xO_2$

For the purpose of gaining insight into the effects of the nonstoichiometry and of the Ti-doping on electrical properties, the relationship between stoichiometry and conductivity was studied in detail.

Large single crystals of $NbO_2$, $NbO_{2+x}$ with $x \simeq \pm 0.1$ and $Nb_{1-x}Ti_xO_2$, $0 \lesssim x \leq 0.6$ have been grown by the Czochralski-Kyropoulos technique in a tri-arc furnace. Details of the equipment and methods of operation are described earlier in Sect.II. Analysis of the starting materials by spectroscopic techniques showed the following impurities in part per millions.

- For Nb metal — Ta < 100, Fe ~ 2, Ca < 1
- For $Nb_2O_5$ — Ta < 50, Si < 1, Ca < 1, Al < 1
- For $TiO_2$ — Si ~ 5, Na ~ 3, Mn ~ 1, Ca < 1
- For Ti metal — Si ~ 8, Fe ~ 3, Na ~ 1, Mn < 1

Laue photographs showed that crystals pulled without the benefit of a seed all had more or less the same orientation, with the growth direction inclined by about $16^\circ$ to the c-axis. However when oriented seeds were used, it was possible to grow large crystals, typically 1. x 3/8 inch, with an orientation differing from that of the seed by no more than $5^\circ$. It proved easier to grow crystals with c-axis orientation than crystals with a-axis orientation, and the latter often developing twinning. However with proper seeding and necking, both c-axis and a-axis growth are possible. A typical crystal is shown in Fig. IV-1.

Spectroscopic analysis showed that the crystals grown by this method contained no new impurity and that the impurity level was no greater than in the starting materials. In addition, thermogravimetric analysis carried out on pieces taken from various places in the lengths of the boule indicated

excellent homogeneity and a control of the stoichiometry x = O/Nb better than 0.1%. In a recent article, T. Sakata[4] claims that crystals grown in arc-melting furnaces are highly stressed and therefore fragile and unsuitable for physical measurements. A standard micrographic investigation of our samples did not reveal any telltale microcracking, inclusions, or poly-crystalline areas, and the Laue photographs exhibited very sharp, well defined spots indicative of a low density of random microscopic defects. Furthermore, for the purpose of Raman studies partially reported elsewhere[5] uniaxial stresses of the order of $10^{10}$ dynes/cm$^2$ were applied to our crystals without damage. Consequently, we consider Sakata's position as to the quality of arc grown $NbO_2$ single crystals unjustified.

The transport properties of stoichiometric single crystal $NbO_2$ have been reported elsewhere[6]. It was demonstrated that the mobility in the low temperature phase ($T < 1070^{\circ}K$) could be described in terms of small polarons. This indicates a localization of the single 4d electron of the $Nb^{4+}$ ions via a pairing along the c-axis, stabilized by a lattice distortion. Clearly ionic vacancies, such as non-stoichiometry would generate on the Nb or the O sub-lattices, will allow local lattice relaxations destabilizing the Nb-Nb pairs and increasing the conductivity. This is in effect very similar to what temperature does when it induces thermal vibrations in which the maximum amplitude of vibration is of the order of the lattice distortion stabilizing the Nb-Nb pairs, eventually breaking them. Table IV-1 shows our results for single crystals both rich and poor in oxygen. From the behavior of the resistivity it is quite clear that the compositional range of existence extends further than was previously reported[7] and that the departure from stoichiometry does affect at least one transport property, namely the resistivity.

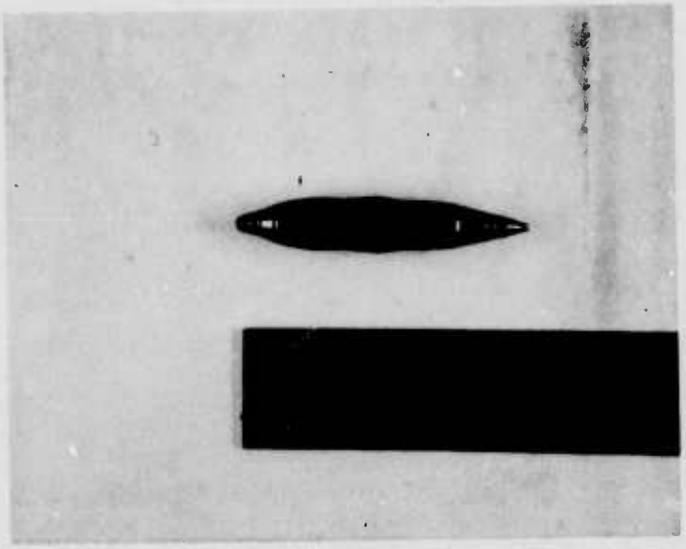

Fig. IV - 1

Typical $NbO_2$ single crystal

TABLE IV-1

Room Temperature Resistivity of $NbO_{2\pm x}$ in Relation to Stoichiometry

| Compositions | Resistivity ($10^4$ ohm-cm) |
|---|---|
| $NbO_{1.90}$ | 0.0438 |
| $NbO_{1.995}$ | 0.7962 |
| $NbO_{2.00}$ | 1.336 |
| $NbO_{2.005}$ | 0.378 |
| $NbO_{2.10}$ | 0.1166 |

The effects of $Ti^{4+}$ doping can in fact be analyzed along the same lines because $Ti^{4+}$ has no d-electrons and breaks a Nb-Nb pair every time it is substituted for $Nb^{4+}$. Consequently for $0. \leq x \leq 0.17$ in the $Nb_{1-x}Ti_xO_2$ system the conductivity increases with x until for $x > 0.17$ the distortion disappears, all Nb-Nb pairs are destabilized and the material has a metallic conductivity. In this respect our results are very similar to the results reported by Sakata[4]. The main difference is that we measure a conductivity four times larger than the conductivity he reports for his polycrystalline samples. This difference is to be attributed to grain boundary resistance.

4) SWITCHING CHARACTERISTICS OF $NbO_2$ SINGLE CRYSTAL: MIXED CRYSTALLOGRAPHIC CONFIGURATION

The switching characteristics under several field conditions have been studied and it has been demonstrated that disorder rather than order could improve switching characteristics in the case of bulk $NbO_2$ single crystal.

In the first experiment we tested the qualitative influence of uniaxial stress in the direction of the applied pulses: in this configuration, we first verified that no switching was observed, whether for "c" or for "a" crystallographic orientations, when no stress was applied. This test was performed with single pulses 1 μsec wide, covering the range 20-2500 V. On the other hand, when samples with either crystallographic orientation were subjected to uniaxial stress, switching was observed in the single pulse mode: i.e. above a certain threshold voltage a sudden decrease of the resistance of the sample could be observed. Without exception, at the threshold value, sparking at or near the surface of the samples took place. A check of the low voltage DC resistance of the samples before and after even a single pulse showed an irreversible change in the form of a decrease from an initial value of about 30 KΩ to a final value of about 3 KΩ. The samples seemed to remain at this level indefinitely. A stereographic microscope

observations at low power showed that between the electrodes there was a distinct visible path in the sample where apparently the sparking took place. Mechanical removal of the path by the use of an airbrasive machine brought back the resistance to its original 30 KΩ value. Repeating the experiment under the same conditions showed reproducible behavior. Even in cases where samples were covered with silicon oil, remarkably enough, sparking occured. The result of this experiment has to be taken only as preliminary since although the samples used were oriented about well-known crystallographic directions, their geometry was not the optimal for this kind of experiment. In order to be able to apply a known stress, the geometry was unsuited. So further experiments are planned in this direction by the use of a well-aligned pressure rig on which one can apply the desired pulses. It has to be noted that the switching took place when the stress was applied in the same direction as the electric field in both "a" or "c" directions.

In the second set of experiments very thin samples were used. All had their "c" axis perpendicular to the surface. One side of the samples had a sputtered niobium film. In one of the experiments, electrodes were placed on the $NbO_2$ surface, along an "a" direction using Viking Alloy and Indium metal with the aid of ultrasonic scrubbing. Under these conditions, again, switching was observed. It has to be noted however that again the need of sparking was obviously present. The final drop of resistance was not by far as dramatic as the one observed in the samples described in our previous report. With this configuration, it can be seen that the actual pulsing takes place on a mixed crystallographic configuration as one can distinguish two different and well-defined paths: the first, a direct, surface line along an "a" direction; the other, through the sample, along the niobium film and again through the sample to the other electrode.

This configuration has the obvious drawback that excitation and switching directions are mixed by the geometry and therefore makes an evaluation of the process very complicated. The oscilloscope tracings are shown in Fig.IV-2 and Table IV-2. Using the same basic samples another experiment was performed: a channel was cut with an airbrasive machine removing a narrow portion of the Niobium sputtered film and leaving the $NbO_2$ surface exposed. Contacts were soldered at both sides of the exposed $NbO_2$ to the Nb film. Since in the past we experienced difficulties with the quality of the contacts, in this case we have to assume that the contacts are of high quality since the bonding between the Nb and $NbO_2$ should be excellent and the soldering with indium to the Nb film presented no problem. Once more, switching was observed in the "a" direction, in a single pulse (or repetititve up to 10 pulses per second), even immersed in silicone oil, but always preceded by the described sparking. The similarity of the results obtained when compared with the "mixed" configuration is remarkable, as can be seen by comparing the oscilloscope pictures taken in both cases as shown in Fig. IV-3 and Fig. IV-2(d).

The third experiment of these series dealt with a well defined geometry. Using a single crystal, a small amplitude AC was applied across the "c" direction of the sample whereas a variable DC bias was established across the "a" direction of the same crystal. The AC response along "c" was then monitored as a function of the DC applied along "a".

In order to make these measurements more defined a circuit was established in a balanced configuration as shown in Fig. IV-4.

The results obtained are plotted in Fig. IV-5 (a) where it can be seen that the resistance (AC) along the "c" direction changes with the applied DC voltage along the "a" direction. As shown in Fig. II-5(b), the resistance (AC) $R_c$ along "c" and the resistance (DC) $R_a$ along "a", scale over most of

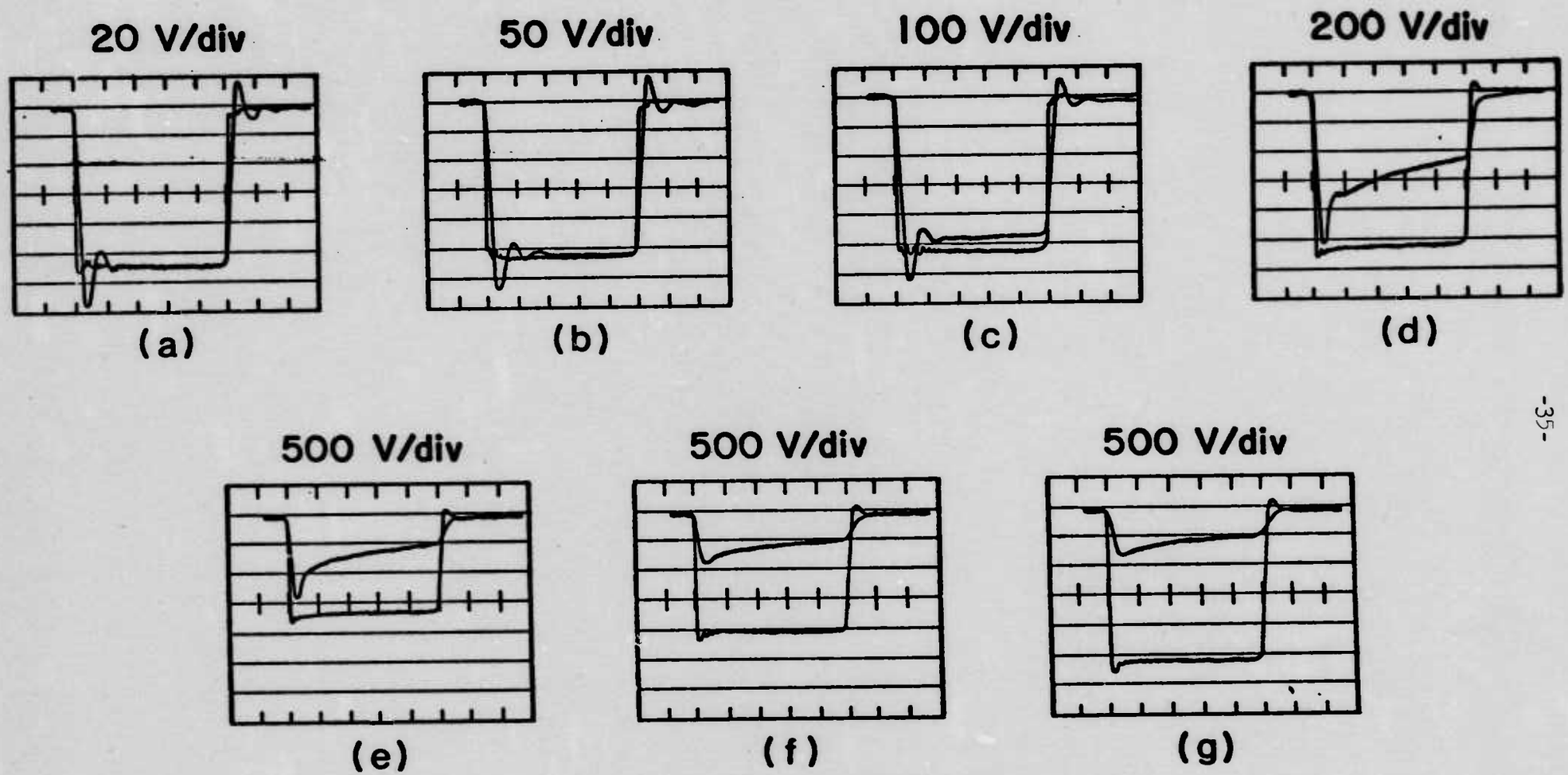
20 V/div
(a)
50 V/div
(b)
100 V/div
(c)
200 V/div
(d)
500 V/div
(e)
500 V/div
(f)
500 V/div
(g)
Horizontal scale: 200 nsec/div
Vertical scale as shown

Fig. IV-2

TABLE IV-2

$NbO_2$ Switching: mixed crystallographic configuration
Single Pulse, 1 μsec Duration

| Fig. | $V_t$ (v) | $V_s$ (v) | $\Delta V$ (v) | I (A) | R (kΩ) | $E_{min}$ (erg) |
|---|---|---|---|---|---|---|
| 1-a | 110 | 110 | - | - | 30 | 4 |
| 1-b | 270 | 260 | 10 | 0.01 | 26 | 26 |
| 1-c | 510 | 460 | 50 | 0.05 | 9.2 | 230 |
| 1-d | 1100 | 420 | 680 | 0.68 | 0.62 | 2800 |
| 1-e | 1650 | 450 | 1200 | 1.2 | 0.375 | 4800 |
| 1-f | 2000 | 400 | 1600 | 1.6 | 0.250 | 6400 |
| 1-g | 2500 | 350 | 2150 | 2.15 | 0.162 | 7600 |

$V_t$ : Total voltage from Velonex pulse generator

$V_s$ : Voltage across sample at end of pulse

$\Delta V$ : $V_t - V_s$

I : Current through sample

R : Resistance of sample at end of pulse

$E_{min}$ : Energy dissipated at the sample, assuming voltage across the sample constant and equal to $V_s$.

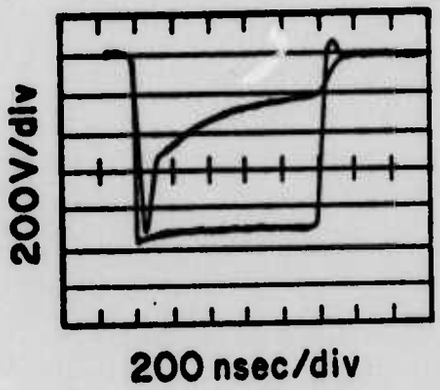


Fig. IV-3
Compare with Fig. IV-2(d)

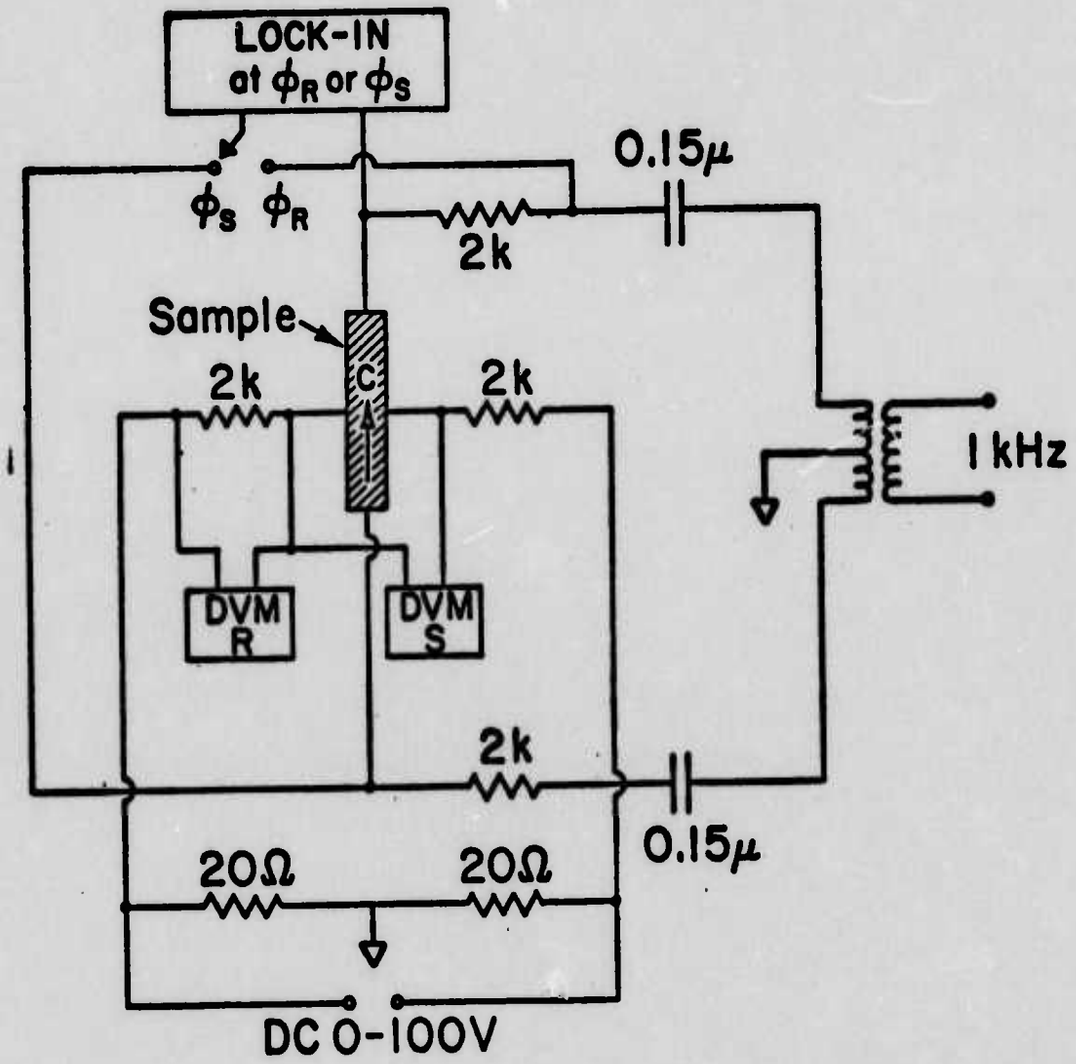
LOCK-IN
at $\phi_R$ or $\phi_S$
$\phi_S$ $\phi_R$
0.15μ
2k
Sample
2k
C
A
2k
1 kHz
DVM
R
DVM
S
2k
0.15μ
20Ω
20Ω
DC 0-100V

Fig. IV-4

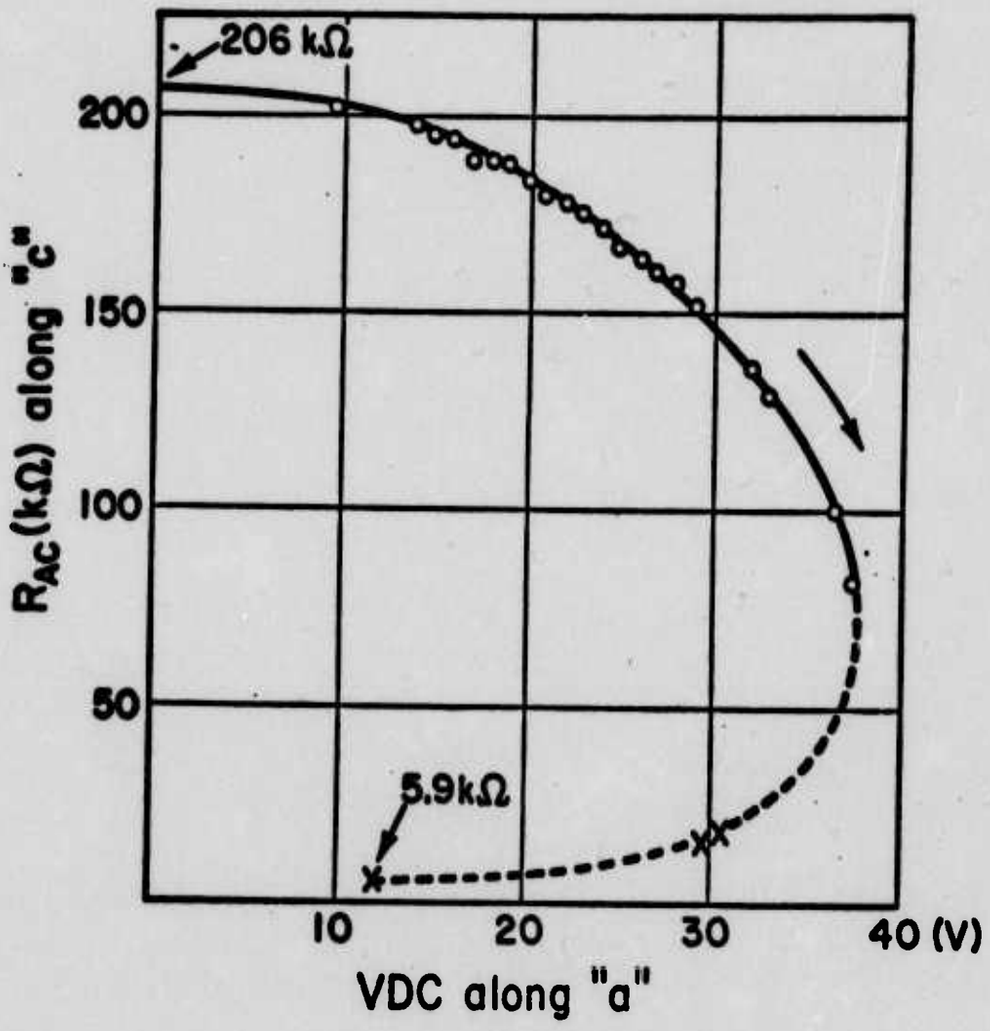
206 kΩ
200
150
100
50
$R_{AC}$(kΩ) along "c"
5.9kΩ
10
20
30
40 (V)
VDC along "a"

(a)

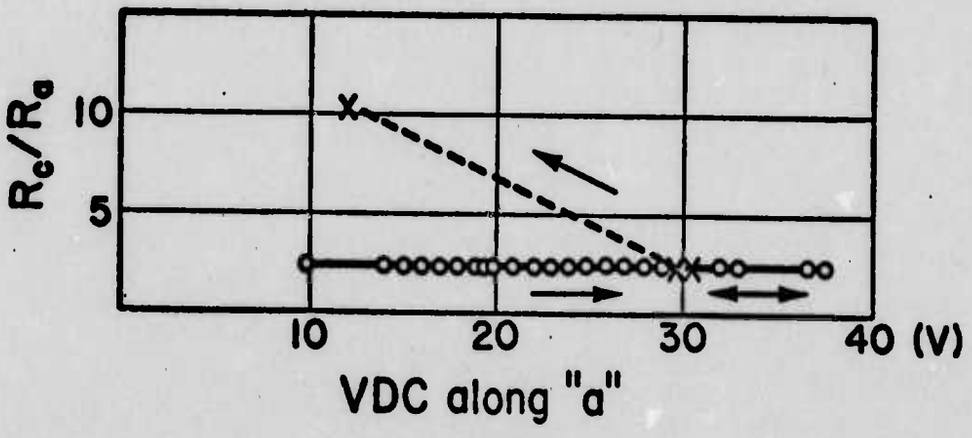
$R_c/R_a$
10
5
10
20
30
40 (V)
VDC along "a"

(b)

Fig. IV-5

the range of bias applied, as would be expected from a thermal phenomena. Above 20 VDC along "a", the measured magnitudes required times of the order of several seconds to reach equilibrium.

A negative resistance region becomes readily apparent as shown in Fig. IV-6. The sudden change in the ratio of $R_c/R_a$ shown in Fig. IV-5 at a nominal power supply voltage above ~ 70 V has yet to be explained. Further work in this configuration is in progress.

Fig. IV-7 shows the phase difference ($\phi_c$) between $I_c$ and $V_c$ in the "c" direction. When the resistance $R_c$ collapses, $\phi_c \rightarrow 0$.

Using samples described above in the second set of experiments (either configuration), a double pulse measurement was performed. In all cases a 10 pulses per second repetition rate was used, with each pulse 400 nsec wide, and variable delay between first and second pulse. The series of oscilloscope pictures in Fig. IV-8 show that complete recovery from the effects induced by the first pulse can be expected only after a time delay of more than 6 μsec. These results were identical, as expected, with the ones obtained from a single shot configuration.

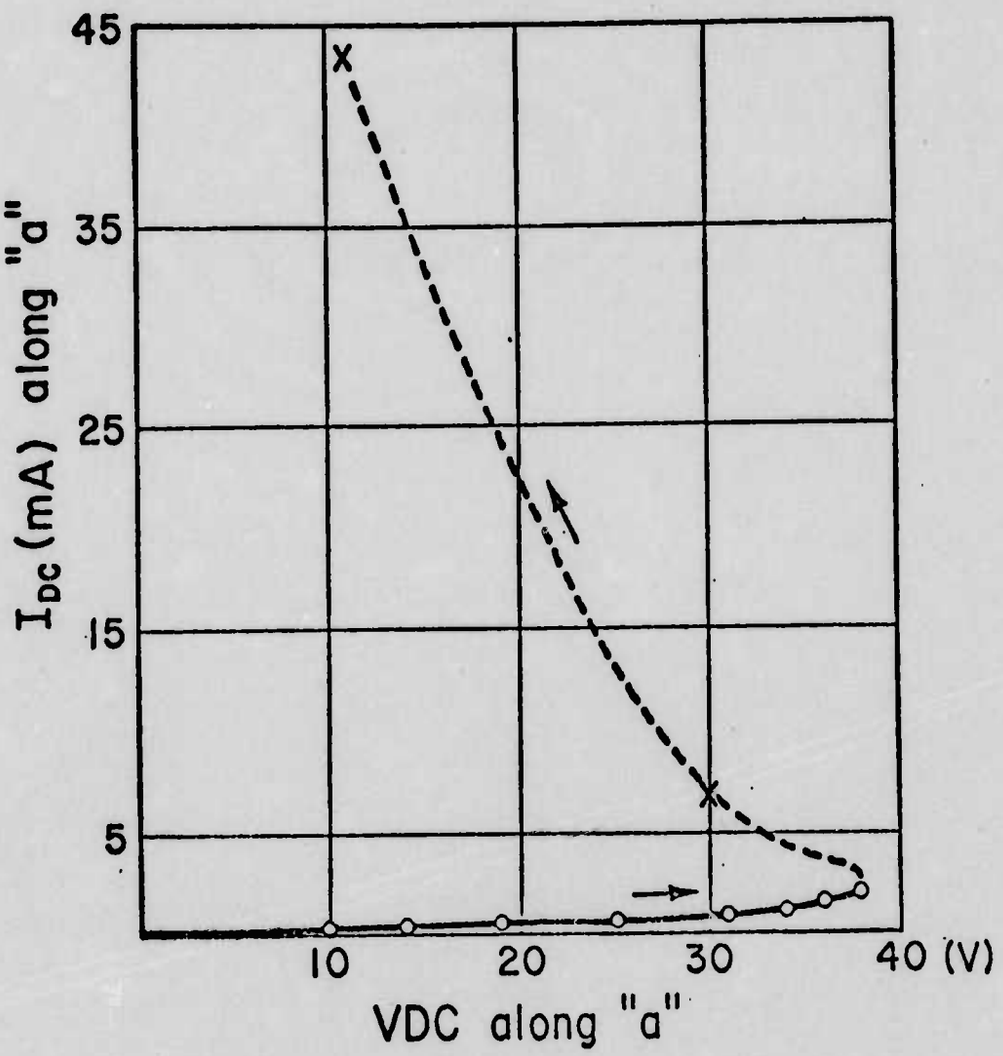


Fig. IV-6

$I_{DC}$(11a) vs. $V_{DC}$(11a)

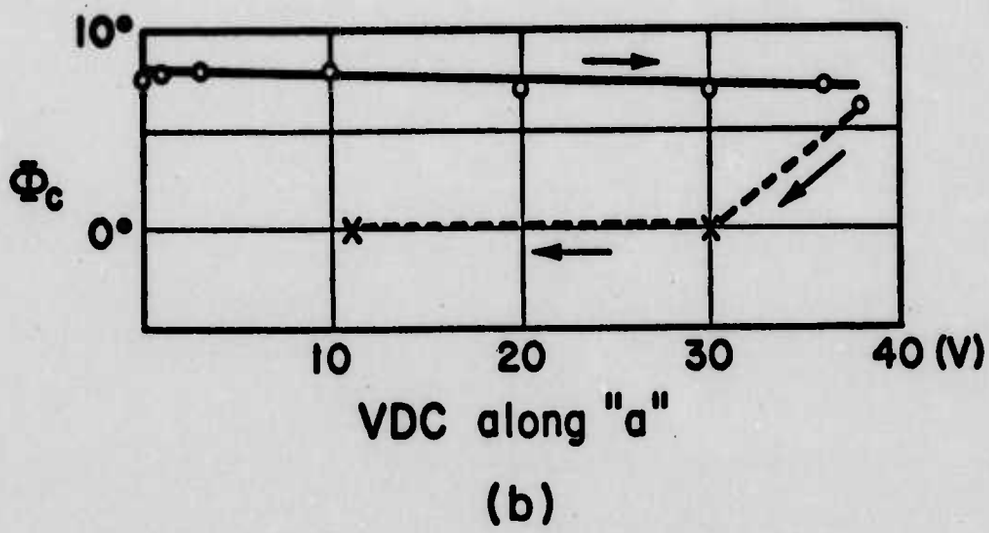


Fig. IV-7

Phase difference $\phi_c$ between $I_c$ and $V_c$ in the "c" direction

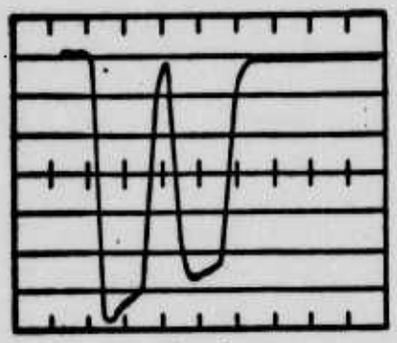

(a)

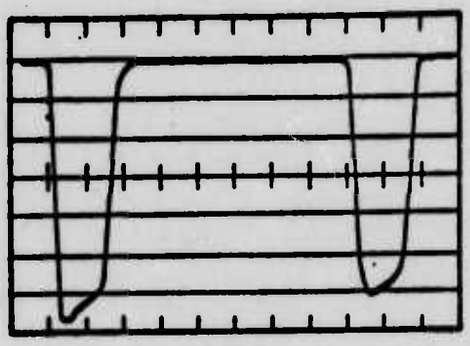

(b)

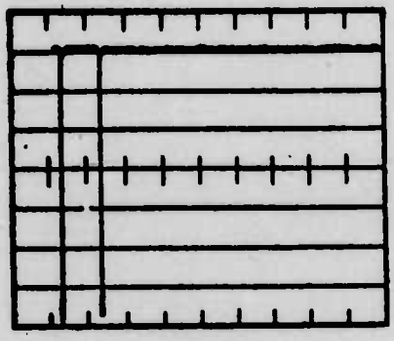

(c)

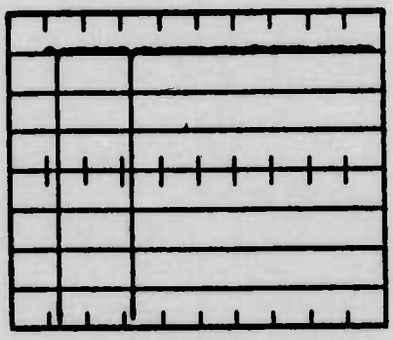

(d)

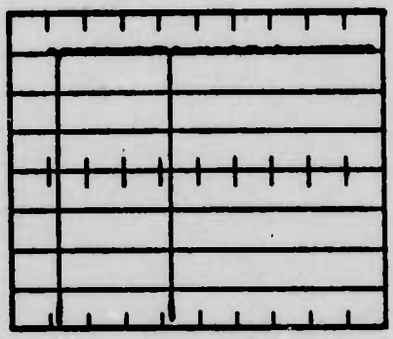

(e)

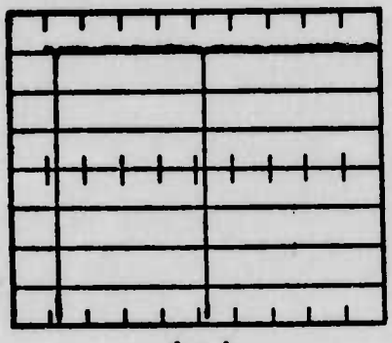

(f)

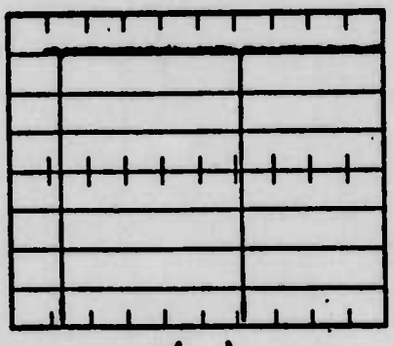

(g)

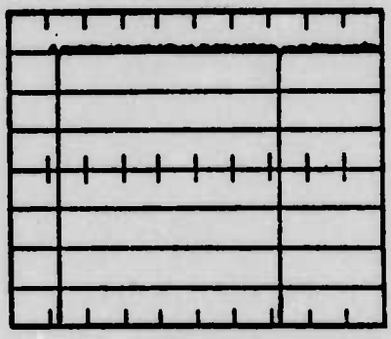

(h)

Vertical scale: 500 V/div

Horizontal scale: (a) and (b) 200 nsec/div

(c) to (h) 1 $\mu$sec/div

Fig. IV-8

## V - POLYCRYSTALLINE $NbO_{1.87}$ (D-TYPE DEVICE)

1) OBJECTIVE

To develop a polycrystalline form of devices capable of shunting transient current up to 80 A , in times shorter than 0.7 ns to meet specific requirements in the development of radiation and thermally hardened switching material for devices. Development goals were optimizing the nonstoichiometry of $NbO_2$, since the switching voltage of nonstoichiometric $NbO_2$ is smaller than that of stoichiometric material.

2) INTRODUCTION

One of the difficulties in the mass production of such a $NbO_2$/NbO device is that the substrate has been obtained using a single crystal technology. While this material grows relatively easily, it is definitely an expensive step.

For this reason, it appeared reasonable to investigate the possibility of using nonstoichiometric niobium dioxide. In the process of studying nonstoichiometric $NbO_2$ we found that polycrystalline material of composition $NbO_{1.87}$ turns out to switch as the first type $NbO_2$/NbO does. The switching voltage is of the order of 170 to 200 volts and switching time when tested by Cpt. Laplante of USAECOM turned out to be the same as before, namely switching times faster than the resolution of the apparatus (about 0.7 ns). In addition, we found that the power handling capability is far better than those $NbO_2$/NbO devices.

3) PREPARATION OF POLYCRYSTALLINE $NbO_{1.87}$ SPECIMEN

Niobium metal and Niobium pentoxide powder produced by Johnson Matthey Chemicals Ltd. was weighed appropriately, pressed into pellets and then melted in a tri-arc furnace. $NbO_{1.87}$ crystal was pulled from the melt using $NbO_2$ single crystal seed. Details of the equipment and methods of operation are described earlier in Section II. The boules weighing several grams each were not single crystalline but denser than the melt. The oxygen gradient along the growth

direction was found to affect the switching threshold voltage. Specimens were cut from two different portions, top (#1) and middle (#2) part of the boule. Both specimens were tested at USAECOM by Cpt Laplante.

4) RESULTS ON POLYCRYSTALLINE $NbO_{1.87}$

The specimen of polycrystalline $NbO_{1.87}$ were cut into approximately cube, 1.2 x 1.2 x 1.16 mm in dimension, and mounted in a 1N23 diode package. The contact was made with tungsten whisker.

i) Threshold voltage

One measurement was made with 6ns pulse width on top and middle cut specimen to determine the variation in threshold voltages with application of a single shot. The measurements of threshold voltage is comparable to those of previous investigations on $NbO_2/NbO$ (Fig.V-1). It appears that the threshold voltage range was less spread compared to that of the $NbO_2/NbO$ devices. In order to attenuate the signals, a 1000:1 probe was used. Therefore all the readings of vertical deflection recorded in the photographs correspond to volts/div. instead of mV/div. as recorded.

ii) Switching times

The switching from the high impedence to the low impedence state occur in times shorter than the resolution of the apparatus ($\ll$ 0.7 ns). Thus switching time is quite similar to that of $NbO_2/NbO$ and these $NbO_{1.87}$ devices exhibit essentially no delay for sufficiently high voltages (Fig. V-2)

iii) Power Handling capability

One measurement was made with 160 ns pulse width and 2000 V (80 A or Amperes limiting), and the other one was made with 1 ms pulse width and 1000 V (11 A limiting). All results are shown in Table V-1.

The polycrystalline $NbO_{1.87}$(#1 specimen) with W-whisker contact could take more than 50 pulses when 160 ns, 2000 volts, (80 A) applied. This is remarkable compared to that of regular $NbO_2/NbO$ devices. At most an $NbO_2/NbO$ device could take only single pulses when contact was made with a tungsten whisker,and eventually melted and shorted to the NbO surface(See

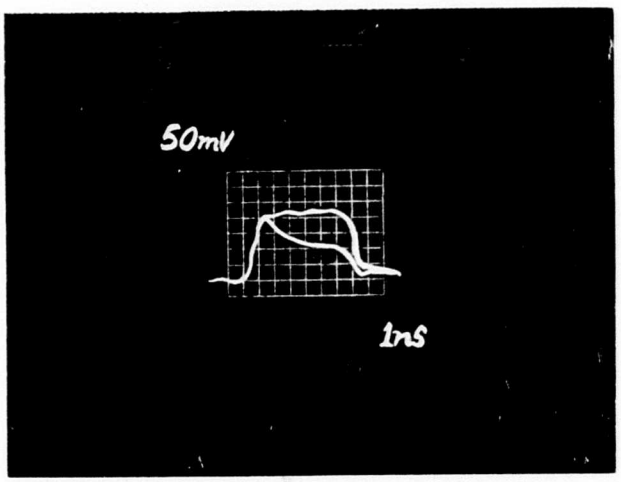


Fig. V - 1

Oscilloscope trace showing threshold voltage in a $NbO_{1.87}$ device under 6 ns pulse width

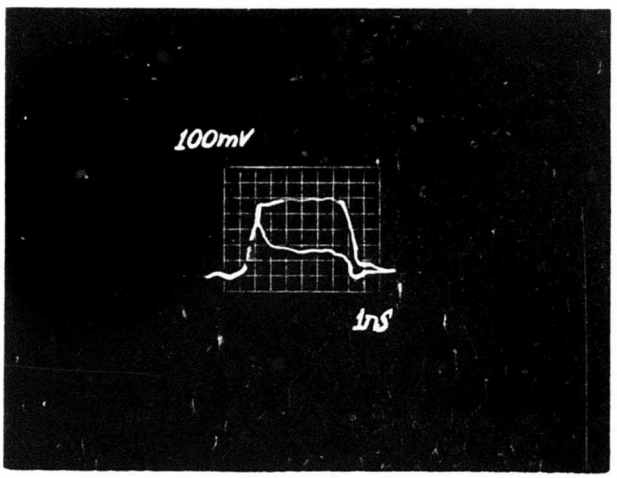


Fig. V - 2

Oscilloscope trace showing fast (< 0.7 ns) switching in a $NbO_{1.87}$ device under 6 ns pulse measurement

TABLE V-1

Threshold Voltages of $NbO_{1.87}$ Devices

| | Thickness | Contact | $V_{th}(1)^*$ | $V_{th}(2)^{**}$ |
|---|---|---|---|---|
| #1 (top) | 0.046" | W-whisker | 260 volts | 35 volts |
| #2 (center) | 0.056" | W-whisker | 170 volts | - |

* $V_{th}(1)$ was measured with 6 ns pulse width

** $V_{th}(2)$ was measured with 160 ns pulse width.

Fig.II-6). However, Cpt Laplante found that if contact was made with a Nb-ribbon (Fig.V-3), the $NbO/NbO_2$ device could take more than 50 pulses with 2000 volt-pulses without serious damage. For 1 ms pulse width, #1 sample with Nb-ribbon contact could take more than 95 pulses with 1000 volts (11 A limiting) again without serious damage. These measurements demonstrated that the power handling capability of the polycrystalline $NbO_{1.87}$ is far better than that of the previous $NbO_2/NbO$ devices.

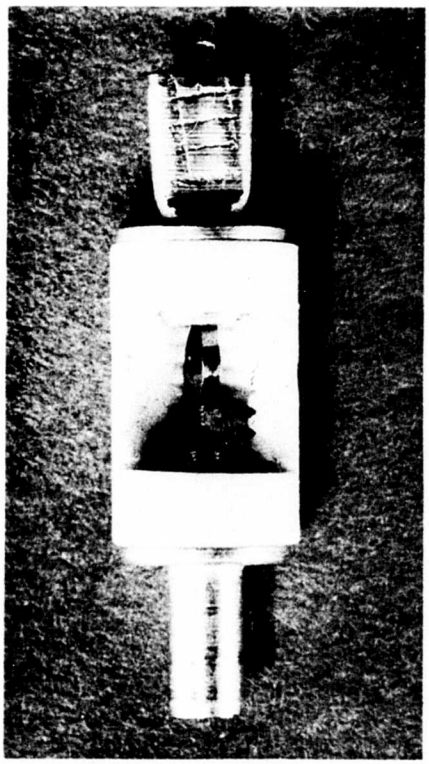

Fig. II - 5(B)

Tungsten whisker in 1N23 microwave diode package was replaced by Nb-ribbon. The $NbO_{1.87}$ polycrystalline device is mounted.

TABLE V-2

Comparison of switching characteristics between $NbO_2/NbO/NbO_2$ (A-type) Devices and $NbO_{1.87}$ (D-type) Devices

| | $NbO_2$ film | $NbO_{1.87}$ [2] (#1) | Remarks |
|---|---|---|---|
| $V_{th}$ (1) [1] (volt) | 240 ~ 500 | 260 | 6 ns pulse W-whisker contact |
| $V_{th}$ (2) (volt) | 40 ~ 60 | 35 | 160 ns pulse W-whisker contact |
| Longevity test (# of pulses) | 1 ~ 2 | >50 | 160 ns, 2KV & 80 A pulses taken by devices W-whisker contact |
| Longevity test (# of pulses) | >50 | - | 160 ns, 2 KV and 80 A pulses taken by devices Nb-ribbon contact |
| Longevity test (# of pulses) | | >95 | 1 ms, 1 KV, 11 A Nb-ribbon contact |
| Switching time (ns) | < 0.7 | < 0.7 | The resolution of the apparatus is ~ 700 ps. |

1 - $V_{th}$ determined by minimum voltage needed to switch device for a 6 ns pulse width. Threshold voltage varies depending on thickness of $NbO_2$ films (1 ~ 10 μm) as well as pulse width

2 - Sample thickness is 0.046"

## VI. SWITCHING PROPERTIES

The field switching properties of $NbO_2/NbO$, stoichiometric and nonstoichiometric $NbO_2$ single crystal have been investigated. These include measurements of transient characteristics on $NbO_2/NbO$ and DC measurements on $NbO_2 \pm x$, $x = 0.1$ as function of current and voltage.

The experimental measurements could be consistently interpreted in terms of the square-root field dependence of the Poole-Frenkel effect.[8] It is hardly necessary to call attention to the fact that consistency does not imply correctness. As more results become available in the future experimentation, the conclusion reached below may be subject to alteration, but at this time, the Poole-Frenkel conduction via small polaron is adequate.

The I-V characteristic of a device, chosen to have a high threshold voltage is shown in Fig. VI-1. The curve was obtained at a different applied pulse voltage (100 ns pulse duration) and all occuring at the same time following pulse applications. For an applied voltage higher than the threshold voltage of 255 volts, the device exhibits the negative resistance behaviour to be expected from materials such as $NbO_2$ capable of undergoing a semiconductor to metallic transition and indicative of a filamentary process. Fig. VI-2 shows a plot of $\ln I$ vs. $V^{\frac{1}{2}}$ showing an electrode limited (Schottky barrier) to bulk limited conduction and then followed by a high conductive state. The values used in this graph are the same as those used before in Fig. VI-1. The graph clearly shows two successive straight lines at the lower values of V and I (see also Fig. VI-11). The points at which the straight lines character are interrupted may well have to do with the

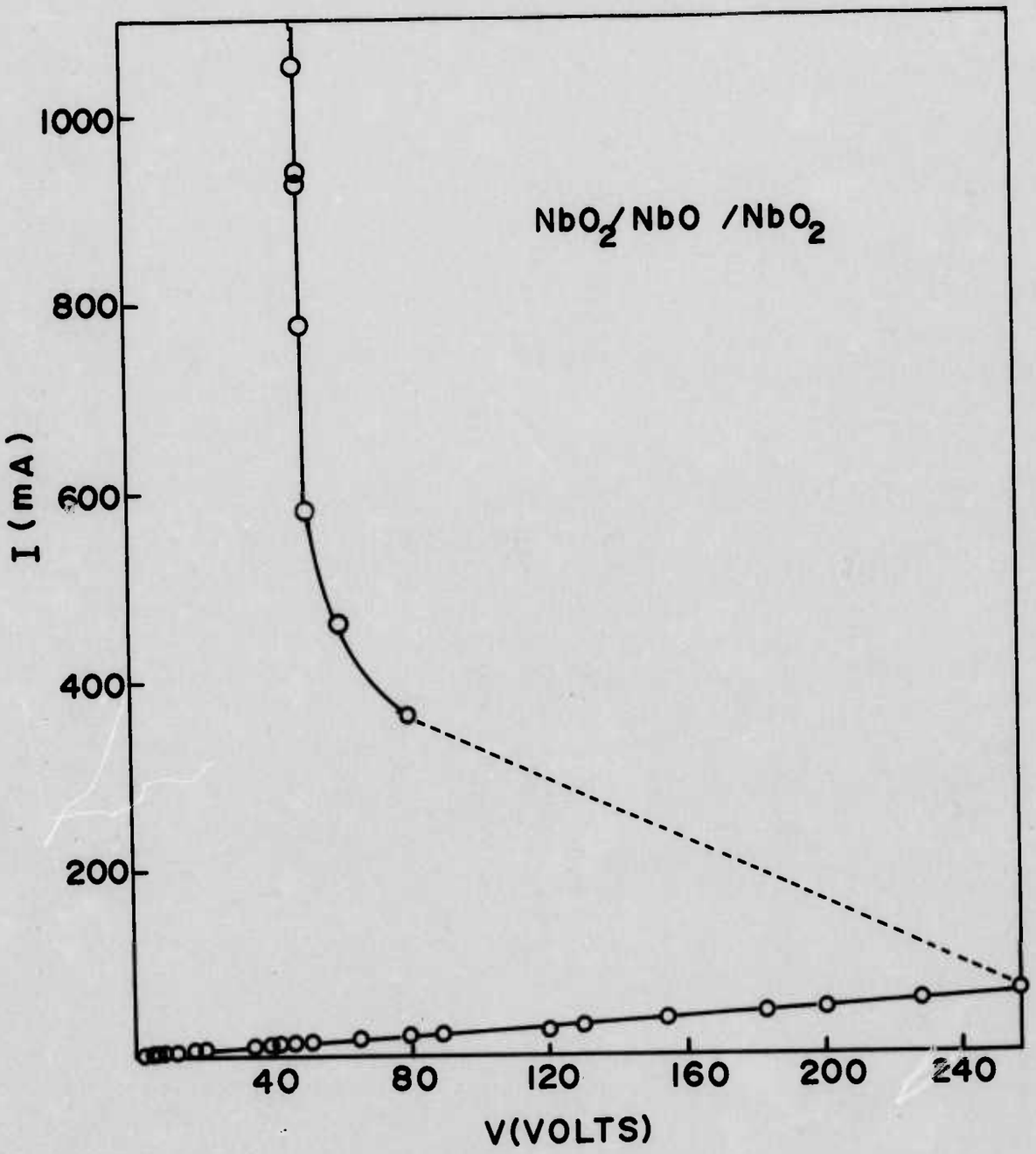


Fig. VI - 1

Current-voltage characteristic of $NbO_2/NbO$ device under pulse condition ($\tau$ = 100 ns)

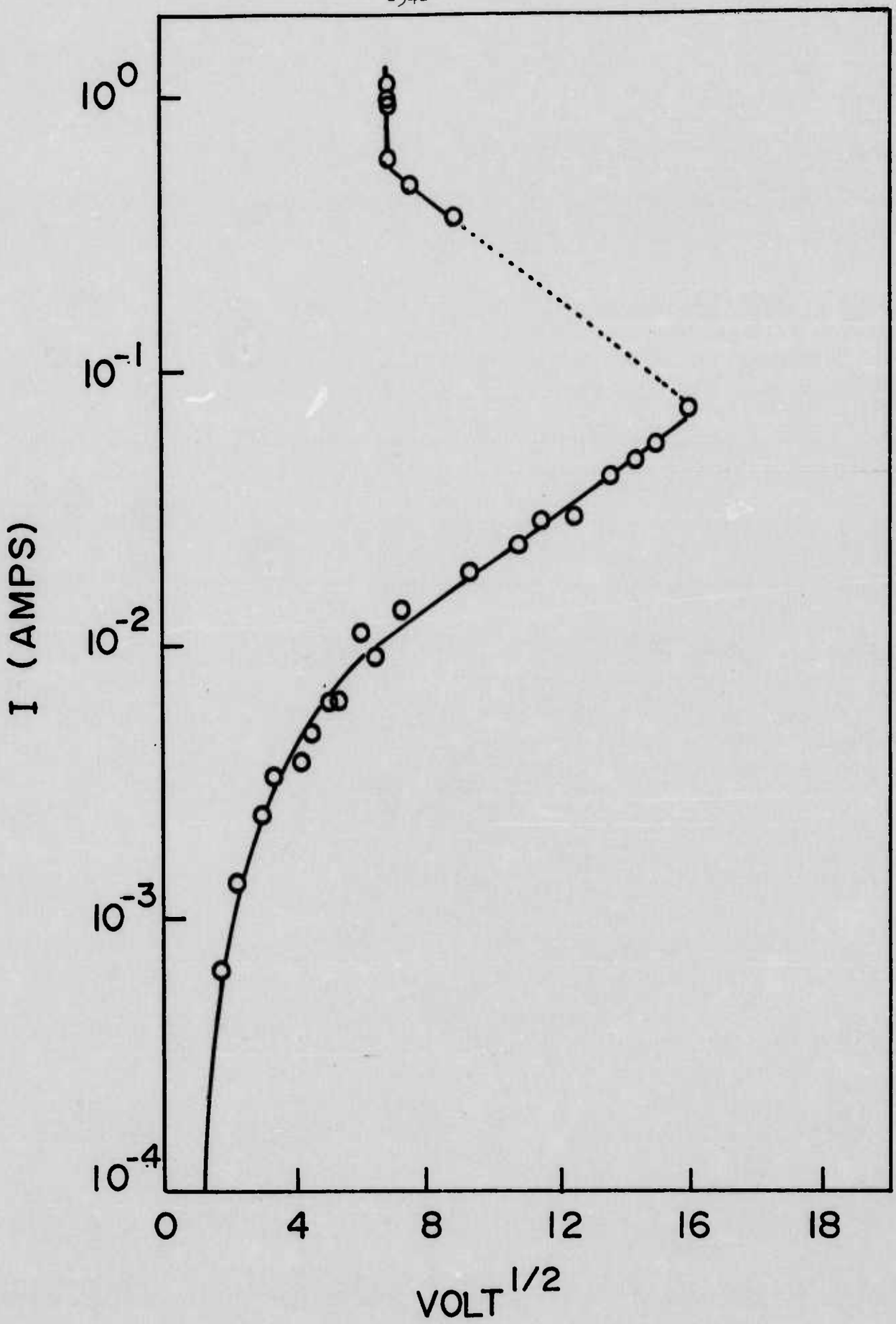


Fig. VI - 2

Linear dependence of log I vs (volt)$^{\frac{1}{2}}$ for $NbO_2$/NbO device

onset of a different mechanism for conduction. The linear dependence of $\ln V$ vs $V^{\frac{1}{2}}$ corresponds to the well known behavior of a Schottky barrier at the junction or Polle-Frenkel effect in the case of bulk material. These will be discussed later in detail, comparing them with d.c. measurements on $NbO_2$ single crystals.

In the past we experienced that there were always discrepancies in threshold voltages between our measurements and those of Capt. Laplante, USA ECOM. However, it was found that the minimum threshold voltage was dependent on the duration of the applied pulse. The variation of threshold voltages $V_{th}$ with measuring time is shown in Fig.VI-4,as plot I vs. V for the same device with $\tau$ = 0.6 $\mu$ to 10 $\mu$sec. Attention is directed to the following features:

1) All the cases show common characteristics switching from a low conduction to a high conduction state, and a negative resistance region becomes readily apparent as shown in Fig. VI-4.

2) Fig.VI-5 shows the apparent parabolic increase in the threshold voltage from 25 volts when pulsed with 10 $\mu$sec pulse duration to over 360 volts when pulsed with 1 ns pulse width. A solid point in Fig. VI-5 was obtained from the average of ten devices measured by Capt. Laplante, USA ECOM (See table II-1). Empirically the following equation was obtained and is shown in solid line.

$$V_{th} = 372\ e^{-\sqrt{t}/25}$$

It was noted that plots of $\log V_{th}$ vs $\sqrt{t}$ yielded a straight line. This is shown in Fig. VI-6.

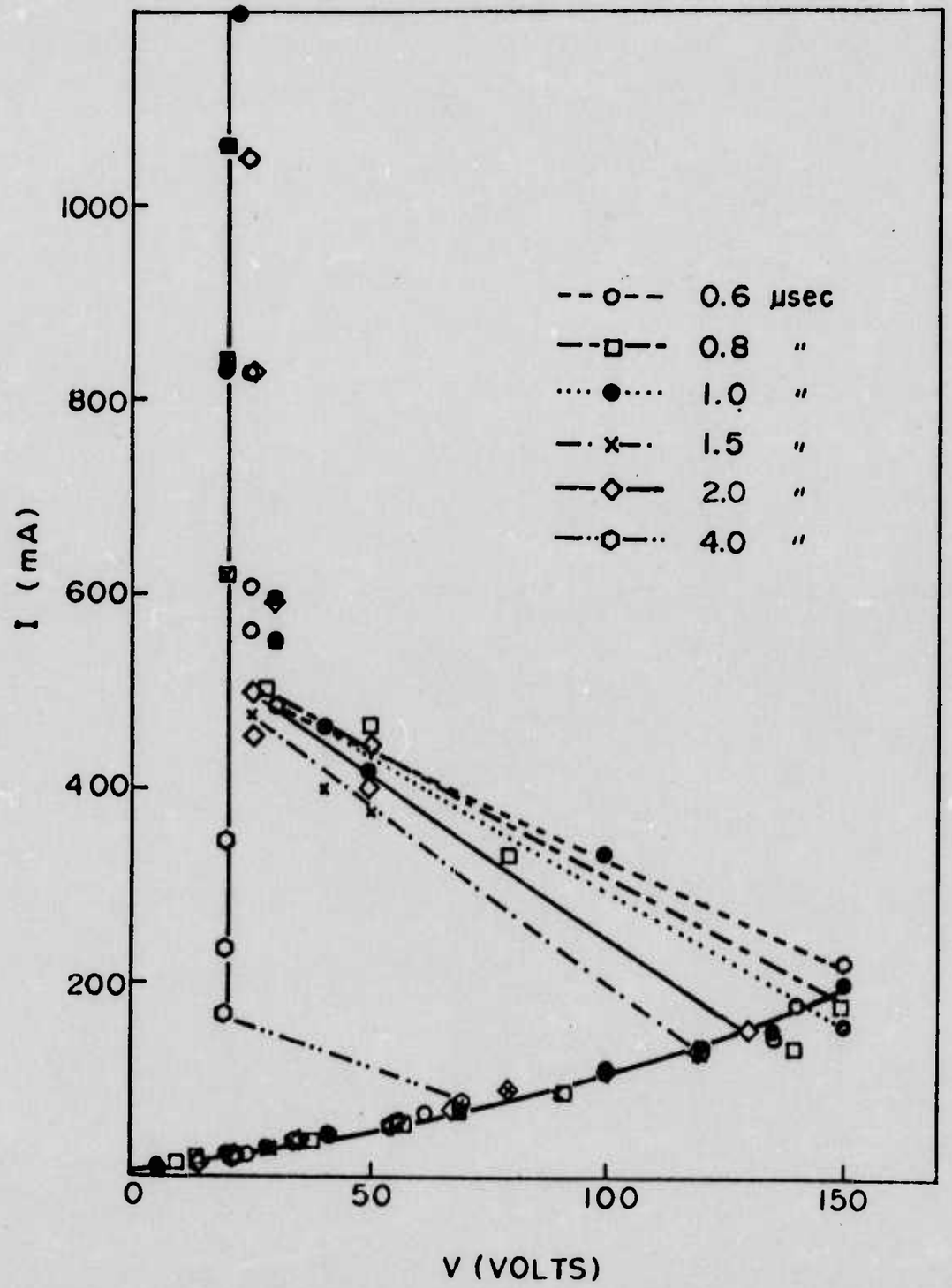


Fig. VI - 3

The variation of threshold voltage versus pulse duration (from 0.6 μsec to 4.0 μsec)

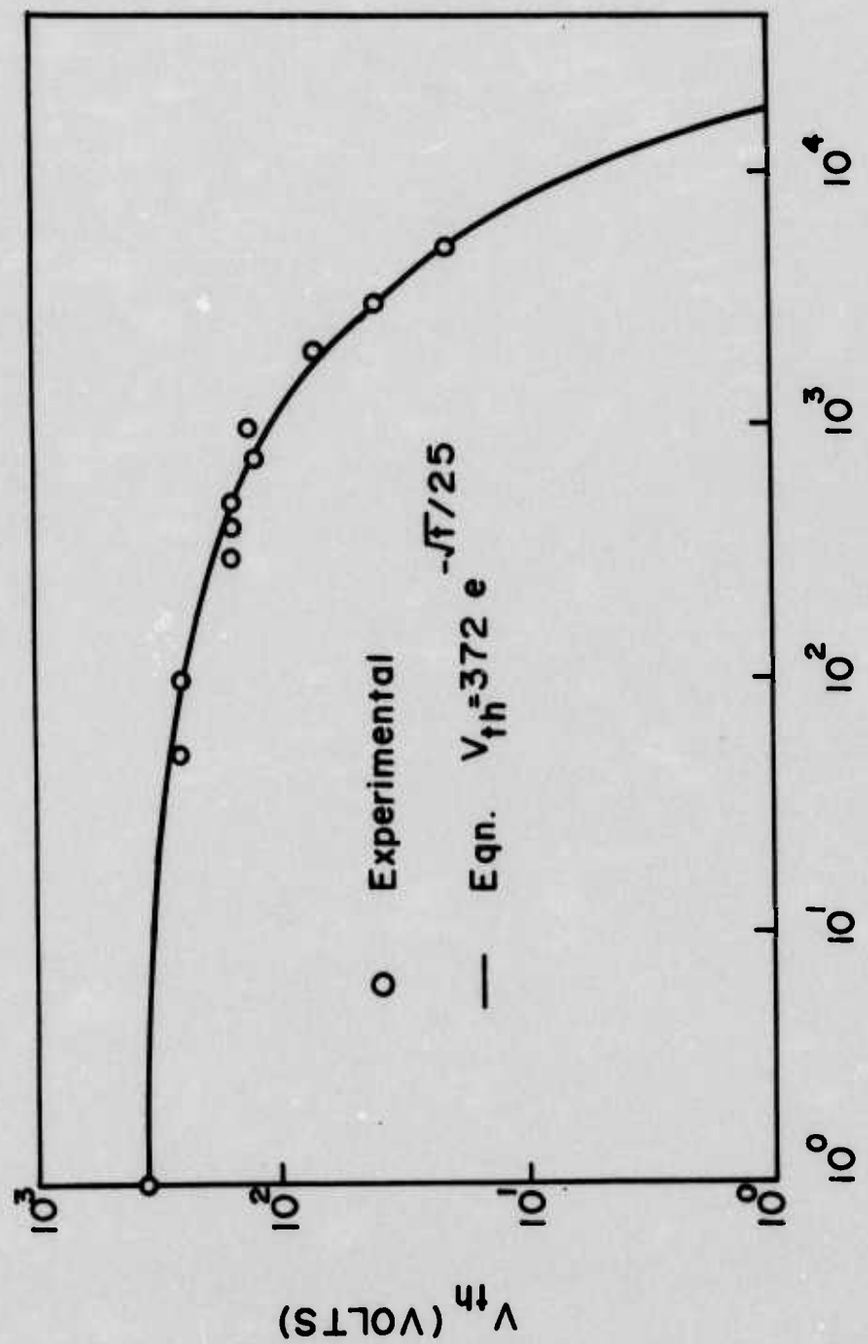


Fig. VI - 4

Threshold voltage ($V_{th}$) vs. measuring time (nsec)

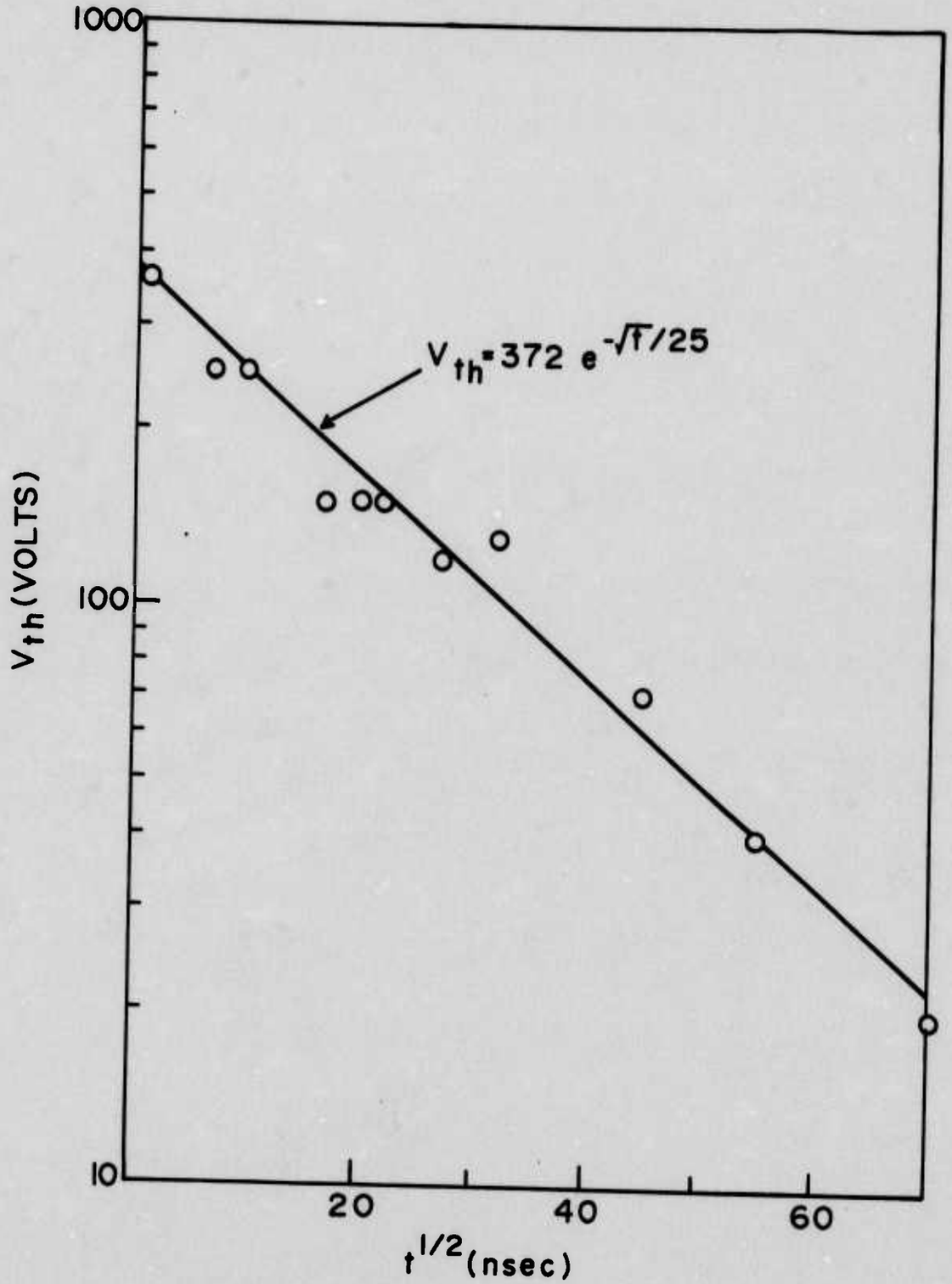


Fig. VI - 5

Threshold voltage ($V_{th}$) vs. $t^{\frac{1}{2}}$(nsec)

3) This switching behavior is quite similar to a semiconductor-to-metallic transition at a threshold voltage $V_{th}$ which decreases with increasing pulse width. For pulse duration $\tau \gtrsim 10$ μsec, the switching is suppressed for this typical device.

4) Inspection shows that in the metallic region, the resistivity under the various pulse duration closely coincide, and the device voltage reduces to about 20-25 volts after switching.

This device behavior under long pulse duration is quite different from that under short pulses ($\sim \leq 5$ ns) described later in detail.

Since we experienced that threshold voltage change with the pulse duration, device characteristics should be examined with fast risetime and high current pulse. They were tested at USAECOM, Fort Monmouth, N.J., using a 50 Ω cable discharge pulser capable of 700 ps risetime resolution, output voltage up to 2 KV (80 Amp) and a nanosecond pulse width. The typical I-V characteristic provided by Capt Laplante is shown in Fig. VI-7.

The difference of the results obtained when compared with the long pulse measurements is remarkable, as can be seen by comparing the I-V curves as shown in Fig. VI-1 and Fig. VI-2. Fig. VI-7 demonstrates that in the high conduction state, the resistivity under the various pulse duration ($\tau \leq 5$ ns) does not coincide at all and the threshold voltage is reduced to significantly lower values with increasing time. However, in all the cases described above, the devices show again some common characteristics, such as electrical switching, negative resistance and nonohmic electrical conduction.

The main difference between short pulse (1 nsec $\leq \tau \leq$ 5 nsec) and long pulse measurements (0.1 μsec $\leq \tau \leq$ 10 μsec.) should be the thermal effect in the case of a long pulse duration. For long pulses, because of temperature variation of the threshold voltage, heating effects might play a role. It was noted empirically that plots of IV vs $t^{1/3}$ yielded a straight line and compared to plotting of empirical equation of

$$IV = 825 \exp(-0.423\, t^{1/3})$$

It is remarkable that short pulse (1ns) as well as long pulse measurements up to 5 μ sec. fit extremely well on a single straight line. This indicates that the heating effect on threshold switching might be excluded up to a 17 μsec pulse, which corresponds to the time limit of our empirical equation. The square root time dependence of threshold voltage implies that up to a 17 μ sec. pulse threshold voltage dependson pulse width, and for a longer pulse become saturated approximately less than IV depending on constant term $\alpha$. We estimated I,V and R at the threshold switching point when t = 0 and t = 5 μ sec. and tabulated in table VI-1. It is very interesting that the threshold current of 2.2 A when t ≈ 0, drops to 0.24 A when t = 5μs sec.

In order to understand the bulk $NbO_2$ switching, we have studied DC measurements using thick $NbO_{2\pm x}$ single crystal specimen with $x \simeq 0.1$. DC measurements were made by applying constant current to the bulk $NbO_2$ specimen in a series with a resistor. Figs. VI-9 and VI-10 illustrate the I-V characteristic of $NbO_{2.00}$ specimen. Specimen were cut into cubes of an approximate 1.3 mm thickness and contact was made by platinum foil between sample and screw.

There are three well defined regions for each specimen with different stoichiometry. For the low current region ($i \lesssim 10^{-5}$ A ) the resistance of the specimen was almost independent of current. Therefore in this region

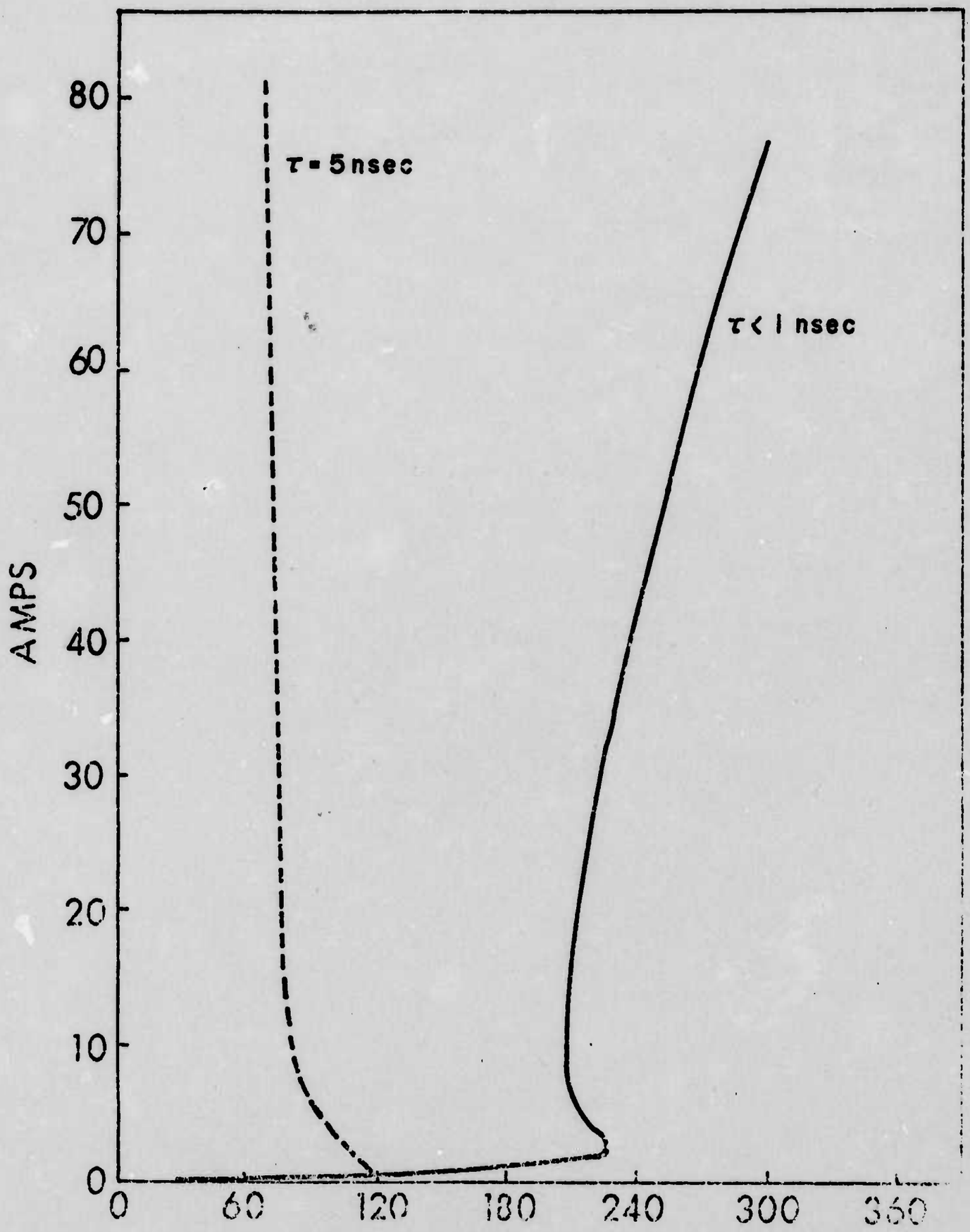


Fig. VI - 6

Current-voltage characteristic of $NbO_2$/NbO device under fast pulse condition ($\tau$ = 5 nsec)

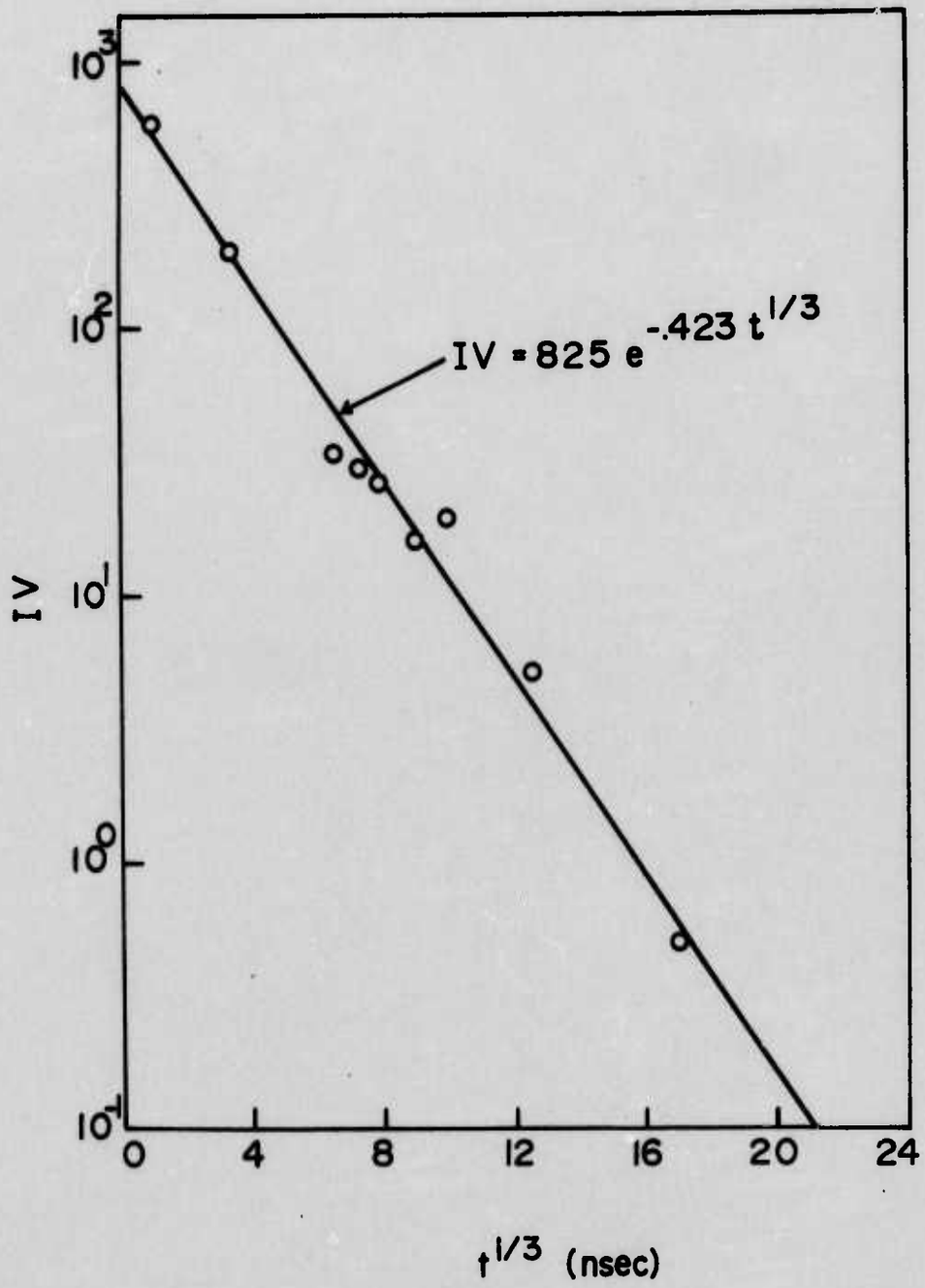


Fig. VI - 7

IV vs $t^{1/3}$ (nsec)

TABLE VI-1.

The estimated current, voltage and resistance of a $NbO_2/NbO$ at threshold switching point.

| | t = 0 | t = S μ sec. |
|---|---|---|
| I (Amp) | 2.2 | 0.04 |
| V (Volt) | 372 | 22 |
| R (Ohm) | 1678 | 550 |

$V_{th} = 372 \exp(-\sqrt{t}/25)$

$IV = 825 \exp(-0\ 425\ t^{1/3})$

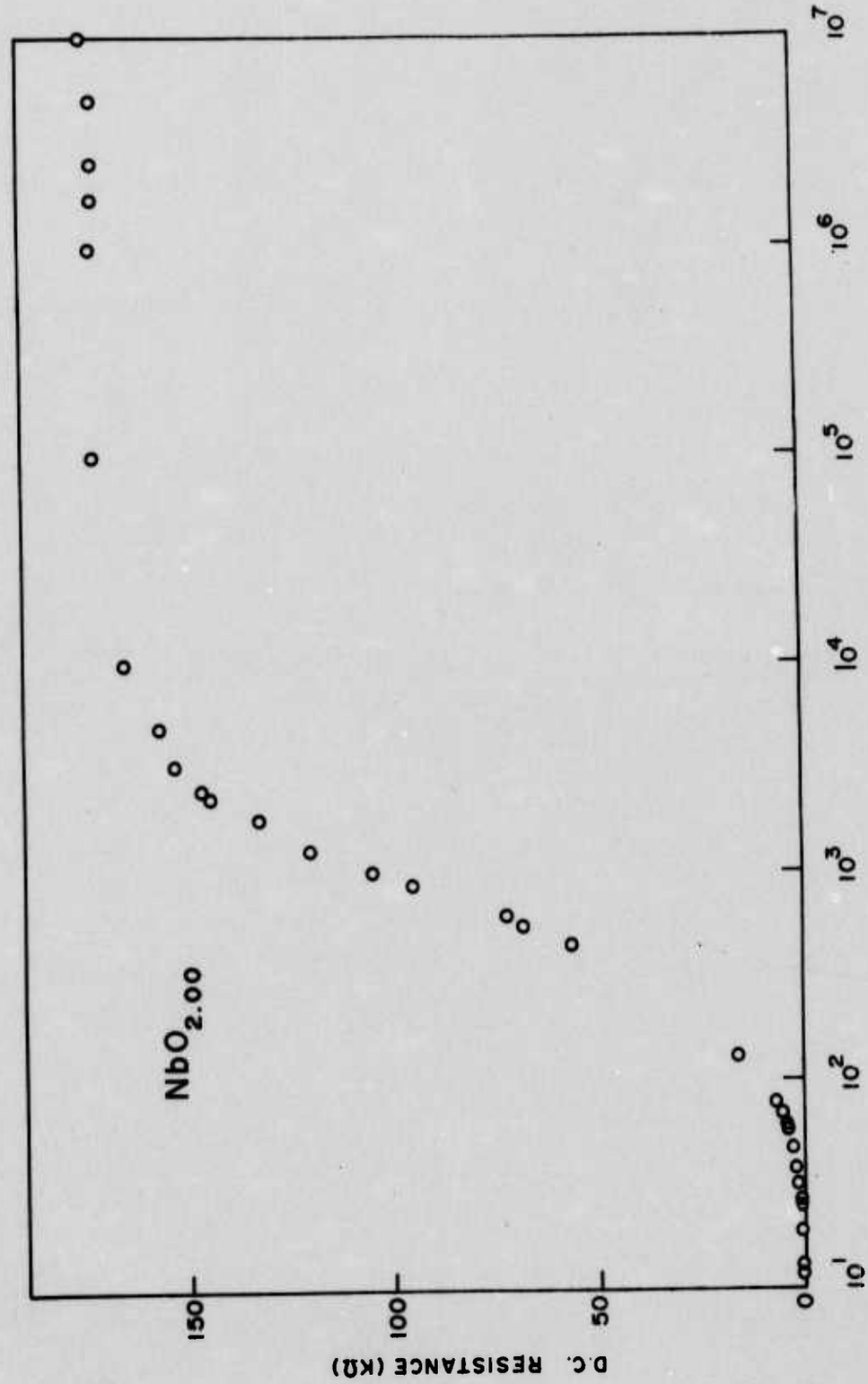


Fig. VI - 8

$R_{DC}$ vs 1/I ($Amp^{-1}$) for $NbO_{2.00}$ single crystal

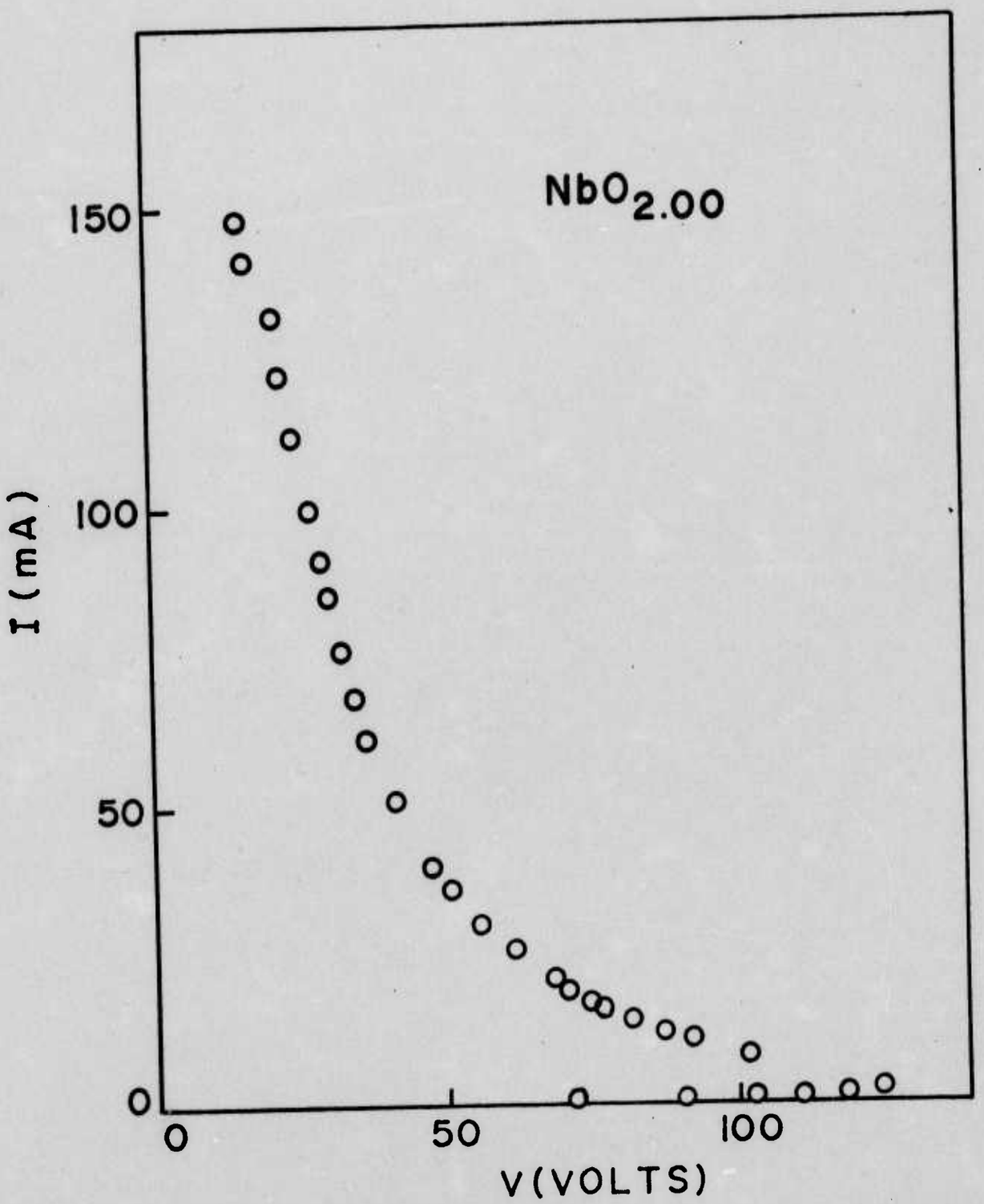


Fig. VI - 9

DC current-voltage characteristic of bulk $NbO_2$ single crystal

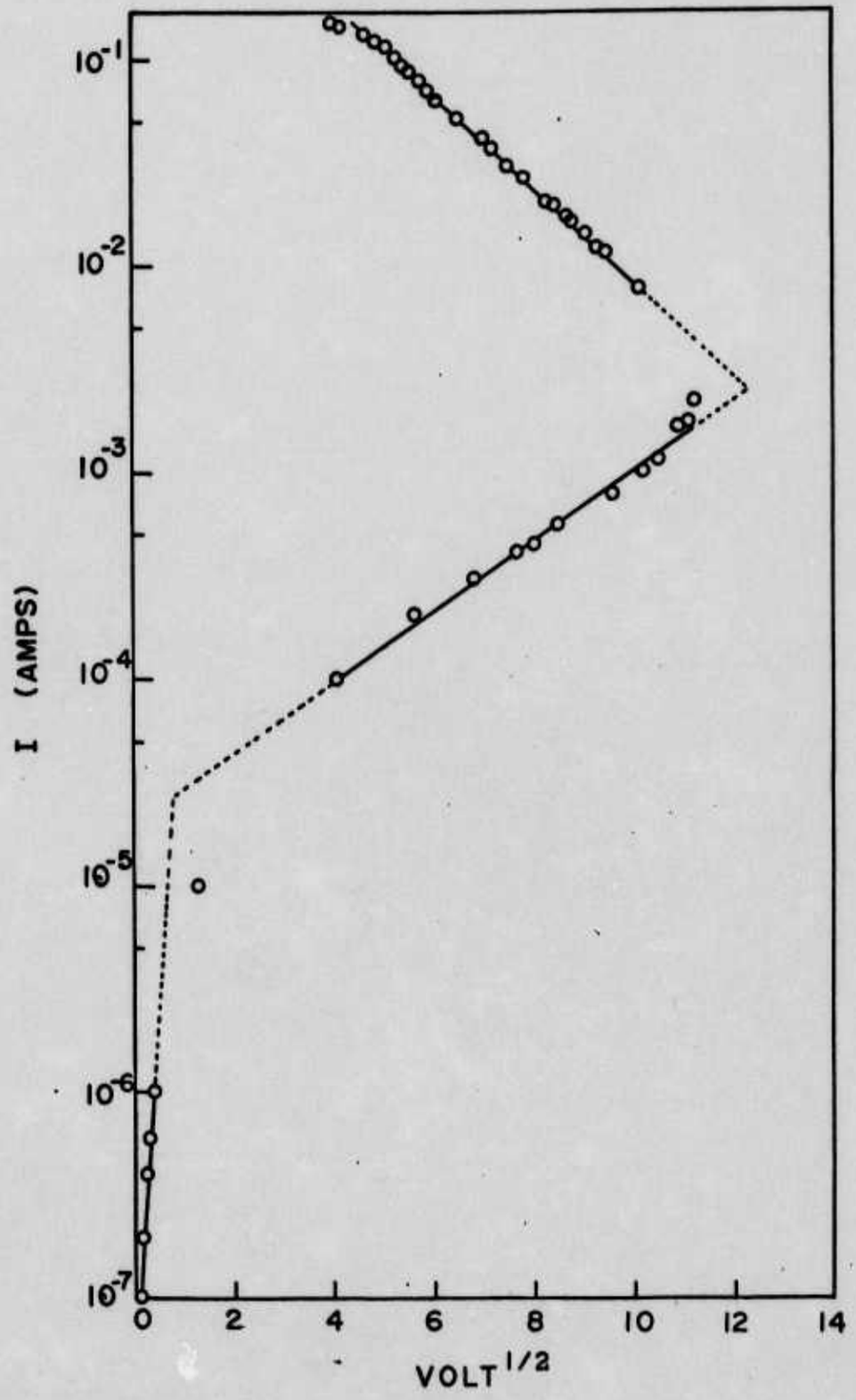


Fig. VI - 10

Linear dependence of log I vs $V^{\frac{1}{2}}$ on $NbO_2$ single crystal

the voltage across the specimen was following the ohmic law. For the intermediate current region (from $10^{-5}$ to $10^{-2}$ A ), the voltage across the specimen increased rapidly, the resistance decreased exponentially and then switched to a high conduction state in I-V characteristic shown in Fig. VI-9 For higher current ($i \gtrsim 10^{-2}$ A to 1.4 A ) the resistance decreases slowly and asymptotically approaches a limiting value (less than 8 ohm-cm) and then becomes a high conduction state. Fig.VI-10 shows a plot of I vs V for $NbO_{2.00}$ specimen. The data used in this figure are the same as the one used before in Fig.VI-9.

The graph clearly shows the similarity obtained by pulse measurements on $NbO_2$ film devices. The point at which switching occured did not coincide with the starting point for decreasing resistance, and it corresponds to the minimum point of the linear portion in Fig.VI-9 This indicates that exponential decrease of resistance is followed by the electrical switching. Therefore, a nonohmic behavior was observed before the switching (definition of pre-switching).

Similar measurements have been done for non-stoichiometric $NbO_2$, such as $NbO_{1.90}$ and $NbO_{2.10}$, and presented in Figs.VI-12 and VI-13. All the results are summarized in Table VI-2.

It is interesting to note that if $NbO_2$ bulk switching is controlled by current rather than voltage switching, current of $Nb_{2.00}$ is the lowest among three different stoichiometries, and it requires less power to switch it. However, DC threshold voltage of $NbO_{2.00}$ is much higher than those of other nonstoichiometric devices. In the past we experienced difficulties with bulk $NbO_2$ switching, since in the case of $NbO_2$ threshold voltage increases with the thickness of $NbO_2$. Since we are interested in low threshold voltage material, it turns out that $NbO_{1.90}$ composition is far better than the other two compositions. Still the threshold voltage of these compositions is too high to switch to a higher conductive state under applied

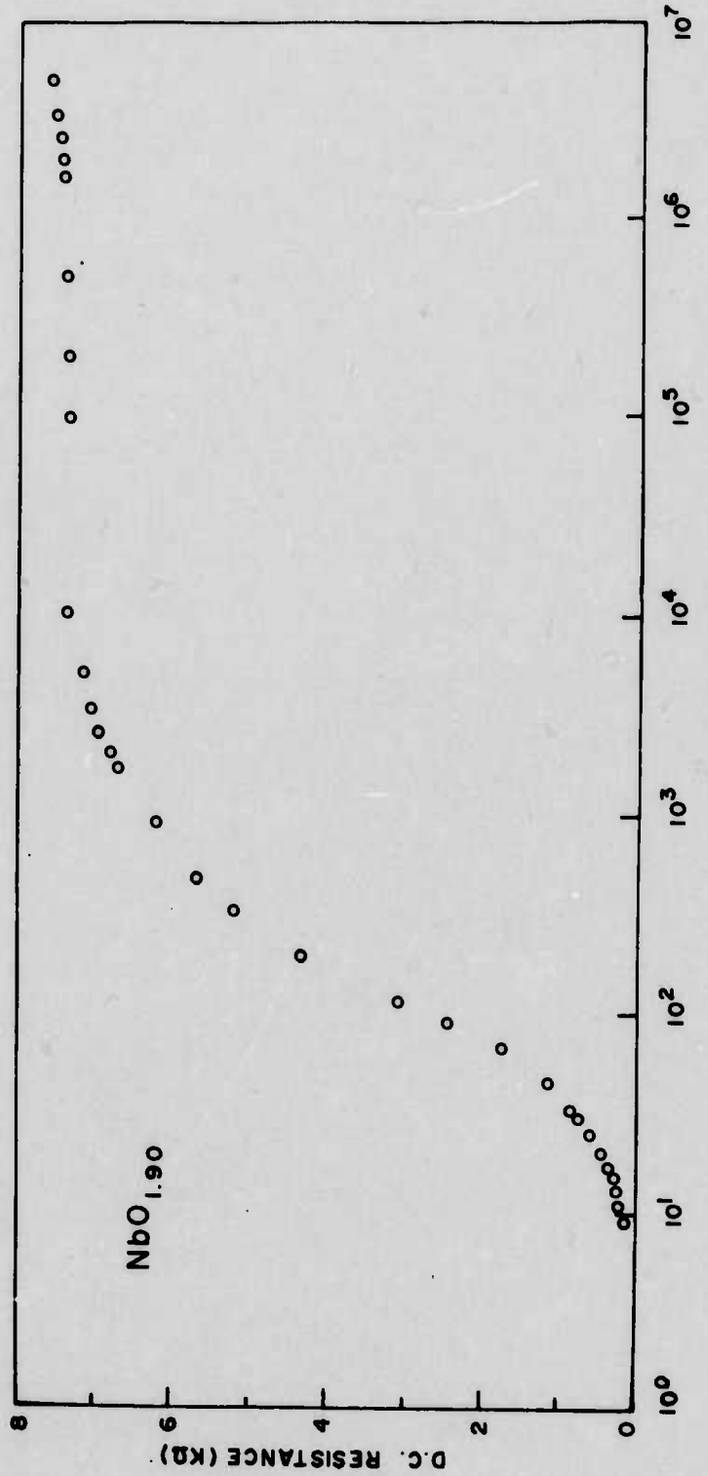


Fig. VI - 11

$R_{DC}$ vs 1/I (Amp$^{-1}$) for $NbO_{1.90}$ single crystal

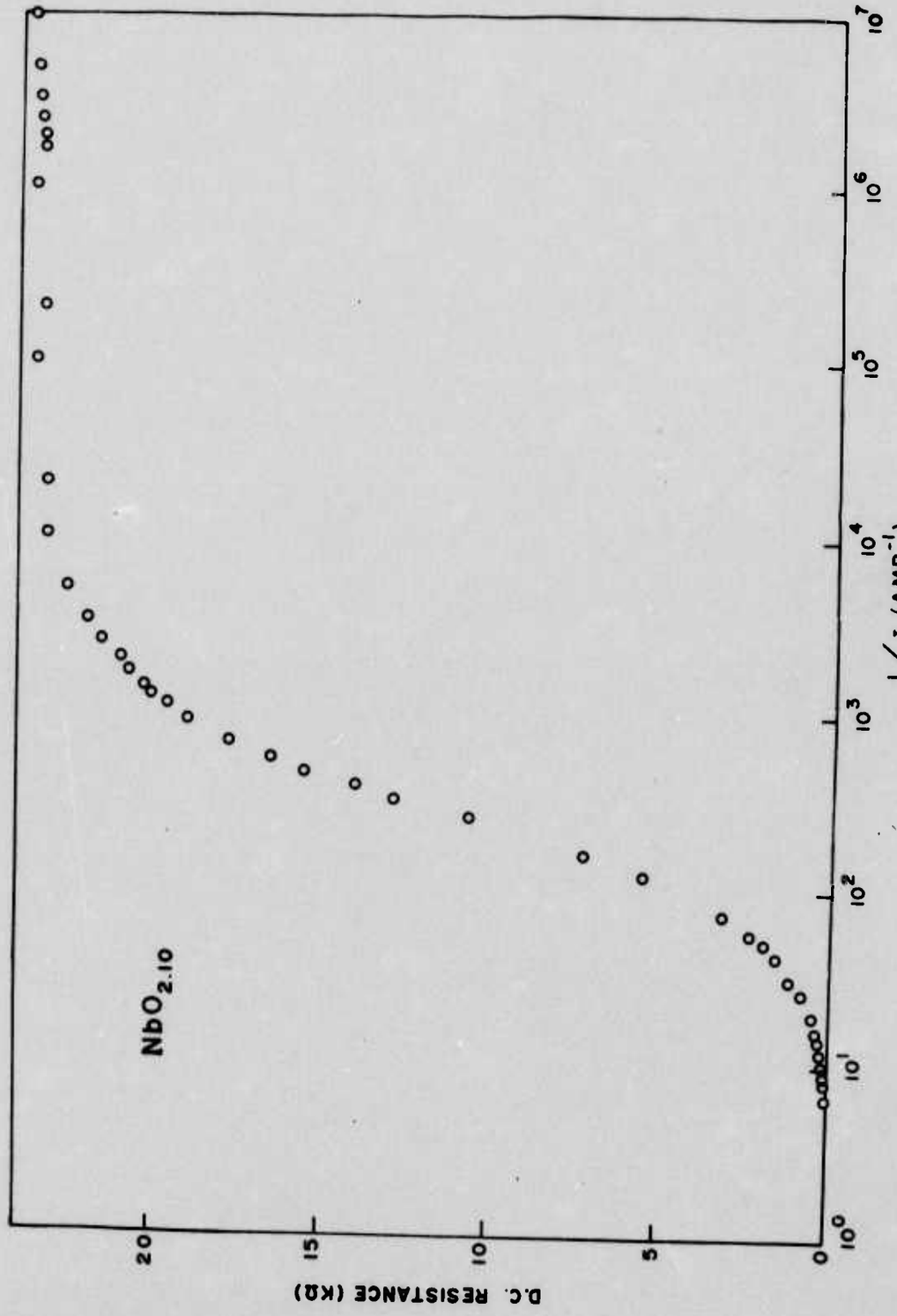


Fig. VI - 12

$R_{DC}$ vs 1/I (Amp$^{-1}$) for $NbO_{2.10}$ single crystal

TABLE VI-2.

DC Measurements of $NbO_{2.00\pm x}$ in relation to Stoichiometry

| | $NbO_{1.90}$ | $NbO_{2.00}$ | $NbO_{2.10}$ |
|---|---|---|---|
| $I_{th}$ (mA) | 11.47 | 2.23 | 8.22 |
| $V_{th}$ (volt) | 28 | 125 | 45.8 |
| $R_{th}$ (KΩ) | 2.44 | 55.9 | 5.56 |
| DC Resistance change between two regions (KΩ) | 8 - 0.15 | 175 ~ 0.10 | 24 ~ 0.12 |
| I (at middle point of curve) (mA) | 0.5 | 0.12 | 0.33 |

pulses. Therefore attempts were made to optimize an appropriate composition to meet the specific requirements as a transient suppressor. For the DC measurements, it is expected that thermal effects will be the most important role for the transition between two regions. We also experienced that for short pulse measurements (1 nsec) the $NbO_2$ layer on the NbO substrate was melted under an intense field (2 KV and 80 Amp). However, short pulse measurements at least minimize the preswitching heating and limit the temperature increase of the device. There is a strong evidence that excludes a theory of thermal switching. When a 3 mm thick $NbO_{1.87}$ sample was pulsed with 6 ns pulse width, it switched faster than that of resolution of apparatus and its threshold was more or less the same as thin $NbO_2$ film (1 to 10 μm). Furthermore, the DC threshold voltage increases more slowly than the thickness of the sample and tends to become almost independent of sample thickness.

Fig. VI-11 shows a plot of log I vs $V^{\frac{1}{2}}$ based on the same data as the one used for the plot of I vs. V in Fig. VI-9 and VI-10. In this figure it can be seen more clearly that all data points fall now in a successive straight line in the "off" as well as "on" state. This region again appears to be consistent with a square root voltage dependence of Schottky effects, as well as the Poole-Frenkel process. After the switching point, logarithmic current increased while the square root voltage across the device decreased. This regime appears to be consistent with a metallic state with a high conduction process.

In summary, there is some experimental evidence of a Schottky barrier as well as the combined effect of two successive regions of square root field dependence on the conduction mechanism. It is worth indicating here that $NbO_2$ material has a second-order semiconductor-to-metallic transition at 1070°K. According to transport measurements summorized in Table VI-3, it

Table VI - 3

Summary of low temperature transport data in niobium dioxide*

| | T = 300°K | T = 435°K | Activation Energy, e.V. |
|---|---|---|---|
| Current parallel to the a-axis | | | |
| Resistivity, ohm-cm | 3509 | 22.4 | 0.44 |
| Hall coefficient, $cm^3/C$ | 1377 | 13.6 | 0.40 |
| Hall mobility, $cm^2\ v^{-1}sec^{-1}$ | 0.40 | 0.60 | -0.035 |
| Drift mobility, $cm^2v^{-1}sec^{-1}$ | 0.016 | 0.114 | -0.17 |
| $\mu_H \cdot T^{3/2}$, $^oK^{3/2}cm^2\ v^{-1}sec^{-1}$ | 2045 | 5365 | -.083 |
| Polaron density, $cm^{-3}$ | $1.11 \times 10^{17}$ | $2.44 \times 10^{18}$ | -0.27 |
| Current parallel to the c-axis | | | |
| Resistivity, ohm-cm | 824 | 11.6 | 0.37 |
| Hall coefficient, $cm^3/C$ | 517 | 6.7 | 0.38 |
| Hall mobility, $cm^2\ v^{-1}sec^{-1}$ | 0.63 | 0.58 | 0.007 |
| Drift mobility, $cm^2v^{-1}sec^{-1}$ | 0.068 | 0.22 | -0.102 |
| $\mu_H \cdot T^{3/2}$, $^oK^{3/2}cm^2\ v^{-1}sec^{-1}$ | 3270 | 5181 | -0.040 |
| Polaron density, $cm^{-3}$ | $1.11 \times 10^{17}$ | $2.44 \times 10^{18}$ | -0.27 |

* data from Ref: 6

has low, anisotropic mobility ($\mu_d(11a) = 0.016$, $\mu_d(11c) = 0.63$ $cm^2/V$ sec) at room temperature and its temperature dependence is interpreted by thermal activation. Furthermore, the ratio of Hall mobility to drift mobility is much larger than one, and the drift and Hall mobilities differ also in their temperature dependence. These transport properties in $NbO_2$ demonstrate that the mobility in the low temperature phase can be described in terms of the small polaron picture.

To begin, it is noted that two successive linear relations for a plot of $\ell n$ I vs $V^{\frac{1}{2}}$ is in excellent agreement with Schottky and Poole-Frenkel law. Particularly the Poole-Frenkel effect in insulators is the field lowering of a Coulombic potential barrier of traps which are positively charged when empty and neutral when occupied by an electron.

Recently Anett and Klein[9] considered some physical origins for neutral traps, and analyzed their field lowering and high field conduction effects in terms of attractive power-law potentials and compared predictions with experimental results. Indeed small polarons provide a possible source of neutral traps. These partially localized electronic states occur under conditions of low electron mobility and strong electron-phonon interaction such that the slow moving electron polarizes the lattice to the extent that a bound state is formed.

Furthermore, Simmon pointed out that it was possible to observe an electrode limited to bulk limited transition in the conduction process if insulators contain a high density of traps.

Since the contact resistance is much higher than that of bulk $NbO_2$, it follows that I-V characteristics will be virtually thickness independent and very steep, as shown in Fig. VI-11. However at some voltage, the contact

resistance falls to a value equal to that of the bulk since contact resistance decreases much more rapidly with increasing voltage than the bulk resistance. Thus at transition voltage, the combined effect of the contact and bulk resistance will appear at the actual characteristic of the junction.

Thereafter, all of the voltage in excess of about 5 volts in Fig. VI-2 (~ 1 volt in Fig VI-11) will fall across the $NbO_2$ layer, and finally the remaining bulk resistance decreases almost exponentially. These field lowering effects on Schottky barrier and high field conduction are then immediately followed by filamentary process thermal runaway. The fast pulse measurements indicate that for 500 V applied pulse voltage, the current rises as much as 78% within 10 ns and over 50% within 2 ns. The voltage across the device dropped from 500 to 250 V within 2 ns. However this does not indicate any time scale for switching, because our devices exhibit essentially no delay ($< 0.7$) for sufficiently high voltages (above threshold) before switching occurs. At this point, this post-switching negative resistance path with an 80% reduction in voltage in the first 10 ns would appear to correspond to a Schottky barrier breakdown and also the bulk-limited conduction process due to the Poole-Frenkel effect. In the region in which switching occurs, a power law $I \alpha V^{1.0}$ is followed abruptly by $I \alpha V^{-1.0}$ after switching. This sudden change in power law might be related with the collapsing of a particular gap as the field lowered the barrier. The reason for this change requires further study.

## VII. Conclusion and Recommendation.

In conclusion, the polycrystalline form of devices ($NbO_{1.87}$) demonstrated experimental evidence to meet the specific requirement of radiation and thermally hardened switching material for devices. This shows a natural substitute for the more sophiscated single crystal technique and promises remarkable speed and power handling capabilities of new devices.

The switching mechanism appears to proceed in two stages which could be electrode limited Schottky barrier breakdown and bulk limited field lowering process of $NbO_2$, then followed by a thermal runaway. Although the $\ln I \sim \sqrt{E}$ behavior covers the large range of current and electric field values, in the high field regime the data is fit to $\ln I \sim E$ or $\ln I \sim E^3$ behavior. The latter process is associated with the conduction mechanism of small polarons.[10] Therefore, the $V_{th} \sim \exp(\sqrt{t})$ relation could be understood via frequency-dependent mobility in $NbO_2$ devices. However, it is somewhat uncertain whether the observed switching should be related to the avalanche breakdown or it should be due to delocalization of small polarons. Switching time of our devices is much faster than that of amorphous material switching and it exhibits essentially no delay for sufficiently high voltages above threshold voltages.[3] And a sudden increase in threshold current of a device with increasing voltage cannot be due to thermal effects and necessarily has to be of an electronic nature. However, a field induced transition would not distinguish whether the transition is thermal or electronic in nature.

More work is needed in order to understand the nature of the processes taking place during switching. In particular, further attention needs to be given to the fact that carrier mobility in $NbO_2$ can be described in terms of small polarons. It would be very interesting to undertake a study of the mobility change as the function of a.c. frequency and electric field. Since a small polaron is due to a lattice polarization and any changes in this local polarization will greatly influence the dielectric constant, a field and temperature dependent dielectric constant might reveal much more information about the details of the mechanism. A mean free path in $NbO_2$ by photoemission measurements would be very useful to distinguish the possible carrier multiplication in the switching process.

## References


1. T.B. Reed, Mater. Res. Bull. 2, 349 (1967).
2. G.V. Chandrashekhar, J. Mayo and J.M. Honig, J. Solid State Chem. 2, 523-530 (1970).
3. G.K. Gaule, P.R. Laplante, S.M. Shin, T. Halpern and P.M. Raccah, Metal-Oxide (MOX), Subnanosecond Transient Suppressors, IEEE Washington Component Conference, April 15, 1975.
4. T. Sakata, K. Sakata, G. Hofer and M. Mariachi, J. Crystal Growth, 12, 88 (1972).
5. S.H. Shin, F.H. Pollak and P.M. Raccah, Bull. Am. Phys. Soc. 19, 536 (1974).
6. G. Belanger, J. Destry, G. Perluzzo and P.M. Raccah, Can. J. Phys. 52, 2272 (1974).
7. R.F. Jannik and D.M. Whitmore, J. Phys. Chem. Solids 27, 1183 (1966).
8. J.G. Simmons, Phys. Rev. 166, 912 (1967).
9. P.C. Arnett and N. Klein, J. App. Phys. 46, 1399 (1975).
10. See, for example, N. Fuschillo, B. Lafevic and B. Leung, J. Appl. Phys., 46, (1975) and references therein.

## DISTRIBUTION LIST

| No. of Copies | |
|---|---|
| | **Department of Defense** |
| 2 | Defense Documentation Center<br>Attn: DDC-TCA<br>Cameron Station (Bldg. 5)<br>Alexandria, Virginia 22314 |
| 1 | Director of Defense Research and Engineering<br>Attn: Technical Library<br>RM 3E-1039, The Pentagon<br>Washington, D. C. 20301 |
| 1 | Director<br>National Security Agency<br>Attn: TDL<br>Fort George G. Meade,<br>Maryland 20755 |
| 1 | Director, Defense Nuclear Agency<br>Attn: Technical Library<br>Washington, D. C. 20305 |
| | **Department of the Navy** |
| 1 | Office of Naval Research<br>Code 427<br>Arlington, Virginia 22217 |
| 1 | Naval Ship Engineering Center<br>Attn: Code 61798<br>Prince Georges Center Building<br>Hyattsville, Maryland 20782 |
| 1 | Director<br>Naval Research Laboratory<br>Code 2627<br>Washington, D. C. 20390 |
| 1 | Commander<br>Naval Electronics Laboratory Center<br>Attn: Library<br>San Diego, California 92152 |
| 1 | Commander<br>U. S, Naval Ordnance Laboratory<br>Attn: Technical Library<br>White Oak, Silver Spring<br>Maryland 20910 |
| 1 | Commandant, Marine Corps<br>Headquarters, U. S. Marine Corps<br>Attn: Code A04C<br>Washington, D. C. 20380 |
| 1 | Communications-Electronics Division<br>Development Center<br>Marine Corps Development and Education Command<br>Quantico, Virginia 22134 |
| 1 | Naval Air Systems Command<br>Code: AIR-5336<br>Main Navy Building<br>Washington, D. C. 20325 |
| | **Department of the Air Force** |
| 1 | Rome Air Development Center<br>Attn: Documents Library (TDLD)<br>Griffiss Air Force Base<br>New York 13440 |
| 1 | Headquarters ESD (TRI)<br>L. G. Hanscom Field<br>Bedford, Massachusetts 01730 |
| 1 | Air Force Avionics Laboratory<br>Attn: AFAL/WR<br>Wright-Patterson Air Force Base<br>Ohio 45433 |
| 1 | Air Force Avionics Laboratory<br>Attn: AFAL/DOT, STINFO<br>Wright-Patterson Air Force Base<br>Ohio 45433 |

## DISTRIBUTION LIST (Continued)

| No. of Copies | |
|---|---|
| | **Department of the Air Force (Continued)** |
| 1 | Recon Central/RSA<br>Air Force Avionics Laboratory<br>Wright-Patterson Air Force Base<br>Ohio 45433 |
| 1 | Headquarters, Air Force Systems Command<br>Attn: DLTE<br>Andrews Air Force Base<br>Washington, D. C. 20331 |
| 1 | Director<br>Air University Library<br>Attn: AUL/LSE-64-285<br>Maxwell Air Force Base<br>Alabama 36112 |
| 1 | Air Force Weapons Laboratory<br>Attn: Technical Library (SUL)<br>Kirtland Air Force Base,<br>New Mexico 87117 |
| | **Department of the Army** |
| 1 | HQDA (DAMI-ZA)<br>Washington, D. C. 20310 |
| 1 | HQDA (DAFD-ZAA)<br>Washington, D. C. 20310 |
| 1 | Office, Assistant Secretary of the Army (R&D)<br>Attn: Assistant for Research<br>Room 3-E-379, The Pentagon<br>Washington, D. C. 20310 |
| 1 | HQDA (DARD-ARP/Dr. R. B. Watson)<br>Washington, D. C. 20310 |
| 1 | Commander<br>U.S. Army Materiel Command<br>Attn: AMCMA-EE<br>5001 Eisenhower Ave.<br>Alexandria, Va. 22304 |

| No. of Copies | |
|---|---|
| 1 | Commander<br>U.S. Army Materiel Command<br>Attn: AMCRD-H<br>5001 Eisenhower Ave.<br>Alexandria, Va. 22304 |
| 1 | Commander<br>U. S. Army Missile Command<br>Attn: AMSMI-RR, Dr. J. P. Hallowes<br>Redstone Arsenal, Alabama 35809 |
| 1 | Cdr, US. Army Missile Command<br>Redstone Scientific Information Center<br>Attn: Chief, Document Section<br>Redstone Arsenal, Alabama 35809 |
| 1 | Commander<br>U. S. Army Weapons Command<br>Attn: AMSWE-REF<br>Rock Island, Illinois 61201 |
| 1 | Commander<br>U.S.Army Combined Arms Combat Development Activity<br>Attn: ATCAIC<br>Fort Leavenworth, Ks. 66027 |
| 1 | Commandant<br>U.S. Army Ordnance School<br>Attn: ATSOR-CTD<br>Aberdeen Proving Ground, Md. 21005 |
| 1 | Commander<br>U.S. Army Intelligence School<br>Attn: ATSIT-CTD<br>Fort Huachuca, Az. 85613 |
| 1 | Commandant<br>U.S. Army Field Artillery School<br>Attn: ATSFA-CTD<br>Fort Sill, Ok. 73503 |
| 1 | Headquarters, U. S. Army Aviation Systems Command<br>Attn: AMSAV-C-AD<br>P. O. Box 209<br>St. Louis, Missouri 63166 |
| 1 | Commander<br>Harry Diamond Laboratories<br>Attn: Library<br>Adelphi, Md. 20783 |

## DISTRIBUTION LIST (Continued)

| No. of Copies | Department of the Army (Continued) |
|---|---|
| 1 | Commander<br>U.S. Army Foreign Science and<br>Attn: AMXST-IS1<br>220 Seventh Street, N.E.,<br>Charlottesville, Virginia 22901 |
| 1 | Commander<br>U.S. Army Foreign Science Div.<br>Attn: AMXST CE Division<br>220 7th Street, N.E.<br>Charlottesville, Virginia 22901 |
| 1 | Commander<br>Picatinny Arsenal<br>Attn: NDB 100, Bldg. 95<br>Dover, New Jersey 07801 |
| 1 | Commander<br>Picatinny Arsenal<br>Attn: SMUPA-RT-S, Building 59<br>Dover, New Jersey 07801 |
| 1 | Commander<br>Frankford Arsenal<br>Attn: W1000-65-1 (Mr. Helfrich)<br>Philadelphia, Pennsylvania 19137 |
| 1 | Commander<br>U. S. Army Materials and Mech.<br>Research Center<br>Attn: AMXMR-ATL, Tech. Library<br>Branch<br>Watertown, Massachusetts 02172 |
| 1 | President<br>U. S. Army Artillery Board<br>Fort Sill, Oklahoma 73503 |
| 1 | Commander<br>Aberdeen Proving Ground<br>Attn: Technical Library, Building 313<br>Aberdeen Proving Ground,<br>Maryland 21005 |
| 1 | Commander<br>Aberdeen Proving Ground<br>Attn: STEAP-TL<br>Aberdeen Proving Ground,<br>Maryland 21005 |
| 1 | Chief, ECOM Field Engineer Office<br>U. S. Army Electronic Proving Ground<br>Attn: STEEP-LN-F (Mr. H. A. Ide)<br>Fort Huachuca, Arizona 85613 |
| 1 | Commander<br>USASA Test and Evaluation Center<br>Fort Huachuca, Arizona 85613 |
| 1 | U. S. Army Research Office<br>Attn: AMXRO-PH<br>P.O.Box 12211<br>Research Triangle Park, N.C. 27709 |
| 1 | U. S. Army Research Office - Durham<br>Attn: Dr. Robert J. Lontz<br>Box CM, Duke Station<br>Durham, North Carolina 27706 |
| 1 | Commander<br>U.S. Army Mobility Equipment R&D Cen.<br>Attn: Technical Document Center<br>Building 315<br>Fort Belvoir, Virginia 22060 |
| 1 | U.S.Army Security Agency Combat<br>DEV ACTV<br>Attn: IACDA-EW<br>Arlington Hall Station, Building 420<br>Arlington, Virginia 22212 |
| 1 | Commander<br>U. S. Army Tank-Automotive<br>Command<br>Attn: AMSTA-RH-FL<br>Warren, Michigan 48090 |
| 1 | Commandant<br>U. S. Army Air Defense School<br>Attn: C&S Dept., MSL Science Div.<br>Fort Bliss, Texas 79916 |

## DISTRIBUTION LIST (Continued)

| No. of Copies | Department of the Army (Continued) |
|---|---|
| 1 | Director<br>U.S.A. Engineer Waterways Experiment Station<br>Attn: Research Center Library<br>Vicksburg, Mississippi 39180 |
| 1 | Commander, Desert Test Center<br>Attn: STEPD-TT-ME(S) Met Div.<br>Building 103, Soldiers Circle<br>Fort Douglas, Utah 84113 |
| 1 | Commander<br>Yuma Proving Ground<br>Attn: STEYP-AD(Tech. Library)<br>Yuma, Arizona 85364 |
| 1 | Commander<br>U. S. Army Arctic Test Center<br>APO, Seattle, Washington 98733 |
| 1 | Commander<br>U. S. Army Tropic Test Center<br>Attn: STETC-AD-TL<br>APO, New York, New York 09827 |
| 1 | Commander<br>U.S. Army Materiel Command<br>Attn: AMCRD-R (H. Cohen)<br>5001 Eisenhower Ave.<br>Alexandria, Va. 22304 |
| 1 | U. S. Army Security Agency<br>Combat Developments Activity<br>Attn: Support Division<br>Arlington Hall Station, Virginia 22212 |
| 1 | Commandant<br>U.S. Army Infantry School<br>Attn: ATSIN-CTD<br>Fort Benning, Ga 31905 |

| No. of Copies | |
|---|---|
| 1 | Commander<br>U.S. Army Logistics Center<br>Attn: ATCL-X<br>Aberdeen Proving Ground, Md. 21005 |
| 1 | Commandant<br>U.S. Army Armor School<br>Attn: ATSAR-CTD<br>Fort Knox, Ky. 40121 |
| 1 | Commandant<br>U. S. Army Field Artillery School<br>Attn: Target Acquisition Department<br>Fort Sill, Oklahoma 73503 |
| 1 | Commander<br>U. S. Army Missile Command<br>Attn: AMSMI-RFG (Mr. N. Bell)<br>Redstone Arsenal, Alabama 35809 |
| 1 | Commander<br>Harry Diamond Laboratories<br>Attn: AMXDO-RCB (Mr. J. Nemarich)<br>Adelphi, Md. 20783 |
| 1 | Commandant<br>U.S. Army Signal School<br>Attn: ATSO-CTD<br>Fort Gordon, Ga. 30905 |
| 1 | Commander<br>U. S. Army Satellite Communications Agency<br>Attn: AMCPM-SC-3<br>Fort Monmouth, New Jersey 07703 |
| 1 | TRI-TAC Office<br>Attn: CSS (Dr. Pritchard)<br>Fort Monmouth, New Jersey 07703 |
| | U. S. Army Electronics Command |
| 1 | MIT-Lincoln Laboratory, Room A-082, Library<br>P. O. Box 73<br>Lexington, Massachusetts 02173 |

## DISTRIBUTION LIST (Continued)

| No. of Copies | |
|---|---|
| | **U. S. Army Electronics Command (Continued)** |
| 1 | Transelco Inc.<br>Box 404<br>Penn Yan, New York 14527<br>Attn: Mr. R. V. Horrigan |
| 1 | General Electric Company<br>Research and Development Center<br>K-1 Met 233<br>Schenectady, New York 12301<br>Attn: Dr.L.M. Levinson |
| 2 | Commander<br>U. S. Army Electronics Command<br>Fort Monmouth, New Jersey 07703<br>Attn: AMSEL-TL-MD<br>Mr. Gerhart Gaule<br>Mr.N.Zellermeyer |
| | **Other Recipients** |
| 1 | Sylvania Electronic Systems - Western Division<br>Attn: Technical Reports Library<br>P. O. Box 205<br>Mountain View, California 94040 |
| 1 | NASA Scientific and Technical Information Facility<br>Attn: Acquisitions Branch (S-AK/DL)<br>P. O. Box 33<br>College Park, Maryland 20740 |
| 1 | Advisory Group on Electron Devices<br>201 Varick Street, 9th Floor<br>New York, New York 10014 |
| 1 | Advisory Group on Electron Devices<br>Attn: Secretary, SP GR on Optical Masers<br>201 Varick Street<br>New York, New York 10014 |
| 1 | Thermophysical Properties Research Cen.<br>Purdue University, Research Park<br>2595 Yeager Road<br>Lafayette, Indiana 47906 |

| No. of Copies | |
|---|---|
| 1 | Ballistic Missile Radiation Anal. Cen.<br>University of Michigan, Willow Run Laboratory<br>Institute of Science and Technology<br>P. O. Box 618<br>Ann Arbor, Michigan 48107 |
| 1 | Defense Ceramic Information Center<br>Battelle Memorial Institute<br>505 King Avenue<br>Columbus, Ohio 43201 |
| 1 | Defense Metals Information Center<br>Battelle Memorial Institute<br>505 King Avenue<br>Columbus, Ohio 43201 |
| 1 | Electronic Properties Information Center<br>Hughes Aircraft Company<br>Centinela and Teale Streets<br>Culver City, California 90230 |
| 1 | Plastics Tech. Evaluation Center<br>Picatinny Arsenal, Building 3401<br>Dover, New Jersey 07801 |
| 1 | Reliability Analysis Center<br>Rome Air Development Center<br>Attn: J. M. Schramp/RCRM<br>Griffiss Air Force Base<br>New York 13440 |
| 1 | Tactical Technology Center<br>Battelle Memorial Institute<br>505 King Avenue<br>Columbus, Ohio 43201 |
| 1 | Shock and Vibration Information Center<br>Naval Research Laboratory (Code 6020)<br>Washington, D. C. 20390 |
| 1 | Vela Seismic Information Center<br>University of Michigan<br>Box 618<br>Ann Arbor, Michigan 48107 |

## DISTRIBUTION LIST (Continued)

| No. of Copies | |
|---|---|
| | U. S. Army Electronics Command (Continued) |
| 1 | Commander<br>U.S. Army Tank-Automotive Com.<br>Attn: AMSTA-RHP/Dr. J. Parks<br>Warren, Mich. 48090 |
| 1 | Director<br>Night Vision Laboratory (USAECOM)<br>Attn: AMSEL-NV-OR (Mr. S. Segal)<br>Fort Belvoir, Virginia 22060 |
| 1 | Chief<br>Missile Electronic Warfare Tech. Area<br>EW Laboratory, U.S.A. Electronics Command<br>White Sands Missile Range,<br>New Mexico 88002 |
| 1 | Chief, Intelligence Materiel Dev. Office<br>Electronic Warfare Laboratory, USAECOM<br>Fort Holabird, Maryland 21210 |
| 25 | Commander<br>U. S. Army Electronics Command<br>Fort Monmouth, New Jersey 07703<br>1 AMSEL-NV-D<br>1 AMSEL-NL-D<br>1 AMSEL-WL-D<br>1 AMSEL-VL-D<br>3 AMSEL-CT-D<br>1 AMSEL-BL-D<br>1 AMSEL-TL-DT<br>3 AMSEL-TL-MD<br>1 AMSEL-TL-M<br>1 AMSEL-TE<br>1 AMSEL-MA-MP<br>2 AMSEL-MS-TI<br>1 AMSEL-GG-TD<br>1 AMSEL-PP-I-PI |

| No. of Copies | |
|---|---|
| 1 | Yeshiva University<br>Belfer Graduate School of Science<br>2495 Amsterdam Avenue<br>New York, New York 10033<br>Attn: Dr. Paul M. Raccah |
| 1 | Rutgers University<br>The State University of New Jersey<br>New Jersey Ceramic Research Station<br>New Brunswick, New Jersey 08903<br>Attn: Professor Edward J. Smoke |
| 1 | Rutgers University<br>The State University of New Jersey<br>Electrical Engineering Department<br>New Brunswick, New Jersey 08903<br>Attn: Dr. Lalevic |
| 1 | Signalite Corporation<br>Division Electro Optical Group<br>Neptune, New Jersey 07753<br>Attn: Mr. Fred R. Huettig |
| 1 | Vernitron Piezoelectric Division<br>A Division of Vernitron Corporation<br>232 Forbes Road<br>Bedford, Ohio 44146<br>Attn: Mr. Glenn N. Howatt |
| 1 | Bell Telephone Laboratories<br>Murray Hill, New Jersey<br>Attn: Dr. M. D. Rigterink |
| 1<br>1 | State University of New York College of Ceramics at Alfred University<br>Alfred, New York 14802<br>Attn: Dr. Amiya K. Goswami<br>Dr. Edward E. Mueller |
| 1<br>1 | Owens-Illinois Inc.<br>South Technical Center<br>1510 North Westwood Avenue<br>Toledo, Ohio 43601<br>Attn: Dr J. M. Woulbrown<br>Mr. L. C. Minneman |